

1 **Monitoring of SARS-CoV-2 variant dynamics in wastewater by digital RT-PCR: from Alpha to**
2 **Omicron BA.2 VOC**

3 Sebastien Wurtzer^{1*‡}, Morgane Levert², Eloïse Dhenain², Heberte Accrombessi¹, Sandra Manco¹,
4 Nathalie Fagour¹, Marion Goulet¹, Nicolas Boudaud³, Lucie Gaillard³, Isabelle Bertrand^{4*}, Julie
5 Challant⁴, Sophie Masnada⁵, Sam Azimi⁶, Miguel Guillon-Ritz⁷, Alban Robin¹, Jean-Marie Mouchel^{2*},
6 OBEFINE SIG, Laurent Moulin^{1*}

7 1. Eau de Paris, Research & Development, 33 avenue Jean Jaures, FR-94200 Ivry sur Seine,
8 France

9 2. Sorbonne Universite, CNRS, EPHE, UMR 7619 Metis, e-LTER Zone Atelier Seine, F-75005 Paris,
10 France

11 3. ACTALIA, Food Safety Department, F-50000, Saint-Lô, France

12 4. University of Lorraine, CNRS, LCPME, F-54000 Nancy, France

13 5. SIAM – STV, Avenue de la courtiere, FR-77400 Saint Thibault des vignes, France

14 6. SIAAP, Innovation Department, 82 Avenue Kléber FR-92700 Colombes, France

15 7. Direction de la Proprete et de l'Eau - Service Technique de l'Eau et de l'Assainissement. Rue
16 du Commandeur, FR-75014 PARIS, France

17

18 ‡ Corresponding author : Sebastien Wurtzer, Eau de Paris, sebastien.wurtzer@eaudeparis.fr

19

20 **Abstract**

21 Throughout the COVID-19 pandemic, new variants have continuously emerged and spread in
22 populations. Among these, variants of concern (VOC) have been the main culprits of successive
23 epidemic waves, due to their transmissibility, pathogenicity or ability to escape the immune
24 response. Quantification of the SARS-CoV-2 genomes in raw wastewater is a reliable approach well-
25 described and widely deployed worldwide to monitor the spread of SARS-CoV-2 in human
26 populations connected to sewage systems. Discrimination of VOCs in wastewater is also a major

27 issue and can be achieved by genome sequencing or by detection of specific mutations suggesting
28 the presence of VOCs. This study aimed to date the emergence of these VOCs (from Alpha to
29 Omicron BA.2) by monitoring wastewater from the greater Paris area, France, but also to model the
30 propagation dynamics of these VOCs and to characterize the replacement kinetics of the majority
31 populations. These dynamics were compared to various individual-centered public health data, such
32 as regional incidence and proportions of VOCs identified by sequencing of isolated patient strains.
33 The viral dynamics in wastewater highlighted the impact of the vaccination strategy on the viral
34 circulation in human populations but also suggested its potential effect on the selection of variants
35 most likely to be propagated in immunized populations. Normalization of concentrations to capture
36 population movements appeared statistically more reliable using variations in local drinking water
37 consumption rather than using PMMoV concentrations because PMMoV fecal shedding was subject
38 to variability and was not sufficiently relevant in this study. The dynamics of viral spread was
39 observed earlier (about 13 days on the wave related to Omicron VOC) in raw wastewater than the
40 regional incidence alerting to a possible risk of decorrelation between incidence and actual virus
41 circulation probably resulting from a lower severity of infection in vaccinated populations.

42

43 **Keywords:** SARS-CoV-2 ; COVID-19 ; variant ; Omicron ; wastewater ; dynamics ; mutation

44

45 **Introduction**

46 The COVID-19 pandemic, caused by severe acute respiratory syndrome coronavirus 2 (SARS-CoV-2),
47 is marked by the continuous emergence of numerous variants (World Health Organization, 2022).
48 Among these, some variants show clear evidences of increased transmissibility, pathogenicity or
49 better ability to escape human immune response induced by natural infection or vaccination (Cele et
50 al., 2022, 2021; Planas et al., 2021; Wibmer et al., 2021). The identification of these variants,
51 designated as variants of concern (VOC) by the WHO (World Health Organization, 2022), is of great

52 importance with regard to vaccine strategy, use of certain therapeutic approaches based on
53 neutralizing monoclonal antibodies, to allow a better understanding of the outbreak dynamics and,
54 more generally, the definition of health policies decided by governments.

55 Over the course of the pandemic, different waves of infections have been reported, each of which
56 was mainly associated with one or more VOC. Currently, five SARS-CoV-2 variants were designated as
57 VOCs (Covariants.org, 2022; World Health Organization, 2022). The Alpha VOC (Pango lineage
58 B.1.1.7; clade 20I) became the dominant SARS-CoV-2 variant worldwide in early 2021. At the same
59 time, the Beta (lineage B.1.351; clade 20H) and Gamma (lineage P.1; clade 20J) variants were also
60 identified around the world. From May 2021, the Delta variant (lineage B.1.617.2, clade 21A)
61 subsequently became dominant and was mainly responsible for the fourth wave observed in France
62 during the last quarter of 2021. At the end of 2021, the Omicron variant (lineage B.1.1.529) was
63 identified in multiple European countries and was designated as a VOC in November 2021 (European
64 Centre for Disease Prevention and Control, 2022). Recently, 3 sub-lineages of Omicron VOC were
65 described based on phylogenetic analysis and were designed BA.1 (clade 21K, the former that
66 defined the Omicron lineage), BA.2 (clade 21L) and BA.3 very minor to date (Covariants.org, 2022).
67 Omicron VOC has a panel of mutations associated with enhanced transmissibility and high potential
68 for vaccine-induced immune escape (Cele et al., 2022). In contrast to previous variants, Omicron VOC
69 is thought to have a lower overall severity in vaccinated populations (Ferré et al., 2022; Maisa et al.,
70 2022). However, Omicron VOC has been reported to induce moderate infections in younger
71 populations, with a notable increase in multi-systemic inflammatory syndrome cases according to
72 French health authorities (Santé publique France, 2022a). Omicron BA.1 VOC has led to an
73 unprecedented global resurgence of infection (7-day rolling incidence > 5,000 cases /100,000
74 inhabitants) during the delta wave in December 2021 in France (Santé publique France, 2022b). In
75 this regard, early warning of Omicron emergence and surveillance of its sub-lineage dynamics must
76 be implemented.

77 In order to meet this high demand for screening, the French testing strategy has changed significantly
78 since January 2022. Thus, antigenic tests alone have become sufficient to make a diagnosis of COVID-
79 19 infection, without confirmation by RT-PCR analysis. Although this approach has made it possible
80 to streamline the workload of medical analysis laboratories in towns and hospitals, the possibilities of
81 performing molecular analyses on these samples, screening by PCR for specific mutations of interest
82 and sequencing, have been greatly affected, leading to a bias in patient recruitment and a potentially
83 partial view of the overall viral circulation and the prevalence of each variant. Identification of the
84 infection dynamics and involved VOCs is of great importance, but if the variants become less and less
85 virulent, the clinical epidemiology may no longer correlate with true viral circulation in the
86 populations.

87 Since the beginning of the pandemic, a complementary epidemiological approach based on fecal
88 shedding of virus and its detection in wastewater has been proposed (Medema et al., 2020a).
89 Although many methodological approaches have been described and a more standardized protocol is
90 required (Ahmed et al., 2021; Bivins et al., 2021b, 2021a), the add-value of this approach has been
91 widely demonstrated through the monitoring of the global viral burden of SARS-CoV-2. In this regard,
92 the European Commission recommendation (EU) 2021/472 of 17 March 2021 called for the
93 establishment of a systematic and harmonized surveillance of the SARS-CoV-2 genome and its
94 variants in raw wastewaters in the European member states (Official Journal of the European Union,
95 2021).

96 The establishment of such a surveillance system is of significant interest in a context of low viral
97 circulation to alert on potential viral emergence or re-emergence. The monitoring of variants,
98 especially VOC, can also be performed in raw wastewater but with some limitations. Sequencing, the
99 most frequently described method (Agrawal et al., 2022a; Crits-Christoph et al., 2021; Fontenele et
100 al., 2021; Pérez-Cataluña et al., 2021; Rios et al., 2021), is complex to perform in wastewater due to
101 the relatively low viral load compared to clinical samples and the potentially degradation and/or

102 fragmentation of the viral RNA in such samples. In addition, the presence of multiple lineages in raw
103 wastewater does not allow the proper assembly of reads to determine the complete sequences of
104 circulating genomes and correct lineage assignment without a complex workflow. Even if the data
105 quantity generated by sequencing is relevant, this methodology is also expensive and time-
106 consuming. To overcome these limitations, targeted and specific RT-qPCR approaches have been
107 proposed to detect certain mutations suggestive of variant presence or functional mutations whose
108 evolution could reveal the spread of variants designated as VOC (Wurtzer et al., 2022). Different RT-
109 PCR methods have been proposed based on either relative quantification of mutations to the total
110 SARS-CoV-2 genomes (Erster et al., 2022; Wurtzer et al., 2022; Yaniv et al., 2021), either on wild-type
111 and mutated allelic discrimination (Graber et al., 2021), quantification of mutations and total
112 genomes by digital PCR (Boogaerts et al., 2022; Caduff et al., 2022; Heijnen et al., 2021; Lou et al.,
113 2022). These approaches have been developed and applied to the emergence of Alpha and Delta
114 VOC. To our knowledge, few data are available regarding the emergence and the dynamics of the
115 Omicron BA.1 and BA.2 VOC (Agrawal et al., 2022b; Ahmed et al., 2022; Chassalevris et al., 2022;
116 Kirby et al., 2022; Smyth et al., 2022) .

117 In this study, the specific monitoring of VOC-suggestive mutations was performed by digital RT-PCR.
118 The objectives were to date the emergence of the Omicron BA.1 and BA.2 sub-variants that have
119 been recently detected in France, but also to model the propagation dynamics of these specific
120 mutations in comparison with open statistical data from the national sequencing program
121 (EMERGEN) of clinical samples (Santé publique France, 2022b). Population replacement kinetics of
122 dominant variants (from Alpha to omicron BA.2) was determined. A comparison of the mutation
123 proportions determined by digital RT-PCR and sequencing of wastewater samples was also
124 performed. In addition, methods of data normalization, including human fecal biomarker, were
125 tested on the data set.

126

127 **Material & methods**

128 **Sample collection**

129 Eight wastewater treatment plants (WWTP) were sampled twice a week in greater Paris area and 7 in
130 other French regions. Sixteen sewers were weekly sampled in Paris, France (See map in
131 Supplementary Figure 1). Twenty-four-hours composite samples (according to NF T 90-90-523-2)
132 were taken by automated samplers. Sampling was based on flow rate, started at 7:00 AM and finish
133 at J+1, 7:00 AM. Samples were taken by suction and collected in a refrigerated polyethylene tank at
134 5°C (+or-3°C). The final collected volume was between 8.7 and 14L. Then samples were carefully
135 homogenized, distributed in a 100mL polyethylene bottle, transported to the laboratories at 4°C and
136 processed in less than 24 hours after sampling.

137 A total of 625 samples from the greater Paris area were analyzed and 72 from other French regions.

138

139 **Concentration methods**

140 All samples from Paris greater area, including WWTP and sewer samples, were processed as
141 previously described (Wurtzer et al., 2020). Briefly, samples were homogenized, then 11 ml were
142 centrifugated at 200 000 x g for 1 hour at +4°C using a XPN80 Coulter Beckman ultracentrifuge using
143 a swing rotor (SW41Ti). Pellets were resuspended in 200 µL of PBS 1X buffer and pretreated for
144 dissociating viruses and organic matter that was then removed from supernatant for improving RNA
145 extraction efficiency, according to the manufacturer's recommendations. Supernatant was then
146 lysed, and total nucleic acids were purified using PowerFecal Pro kit (QIAGEN) on a QIASymphony
147 automated extractor (QIAGEN) and eluted in 50 µL of elution buffer according to manufacturer's
148 protocol.

149 The other samples from WWTP were processed according to an alternative protocol (Bertrand et al.,
150 2021). Briefly, 5mL of raw wastewater were used for nucleic acid extraction using 10 mL of

151 NucliSENS® lysis buffer. A purification step using phenol/chloroform/isoamyl alcohol 25:24:1 could
152 be performed depending on the laboratories. The nucleic acid extraction was continued using 70 µL
153 of magnetic silica beads and the NucliSENS® platforms (easyMAG™ or miniMAG™) (BioMérieux). The
154 nucleic acids were eluted in 50 µL of elution buffer.

155 All nucleic acids were finally purified using OneStep PCR inhibitor removal kit (Zymoresearch)
156 according the manufacturer's instructions and then stored at -80°C until molecular assays.

157 The recovery rate of methods was estimated using bovine coronavirus spiked and the repeatability of
158 the measurement was also evaluated on endogenous PMMoV as previously described (Wurtzer et
159 al., 2022).

160

161 **Molecular quantification by digital RT-PCR**

162 A panel of oligonucleotides was designed using AlleleID software vers. 7 (Premier Biosoft) in order to
163 detect and quantify mutations reported in table 1. Briefly, Alpha and Omicron BA.1 VOC have been
164 reported for sharing a deletion of amino acids H69 and V70 in the spike protein (del 69-70), but
165 Omicron BA.1 VOC can be distinguished from Alpha by an additional synonymous substitution (C/T)
166 at the position 21762 (codon 67 of the spike protein). Delta VOC has been reported carry the L452R
167 mutation in the spike protein. Bioinformatics analyses revealed that Omicron BA.2 variant carried the
168 D61L mutation in the ORF6. In addition, PMMoV genome was also detected using previously
169 described oligonucleotides (table 1).

170 Briefly, total SARS-CoV-2 genomes and mutations were quantified by digital RT-PCR. All samples from
171 greater Paris area were processed using a QIAcuity instrument (QIAGEN). Multiplex reactions were
172 performed using QIAcuity One-Step Viral RT-PCR mastermix (QIAGEN) with 800 nM of each primer
173 and 250 nM of each probe in 26k-Nanoplates according to the manufacturer's recommendations
174 (table 1). In order to improve the detection specificity of single nucleotide polymorphism, the

175 thermal profile included a touchdown step. Briefly, reverse transcription was done at 50°C for 10
176 min, followed by activation step at 95°C for 2 min. Then touchdown was composed by 5 cycles
177 including a 5 sec-denaturation step at 95°C followed by a hybridization/elongation step from 63°C
178 with a decrease of 1°C/cycle for 40 sec. Amplification was done by 45 cycles of incubation at 95°C for
179 5 sec and 58°C for 40 sec. The use of these nanoplates provided a minimum of 24k valid partitions for
180 each sample and an estimated detection limit of 1800 copies/L.

181 Other samples were only processed for the quantifying del69-70 mutation among total genomes
182 using QX200 instrument (BioRad). The ddRT-PCR assays were performed in a 20 µL-reaction mixture
183 containing 5 µL of extracted nucleic acids and 15 µL of One-Step RT-ddPCR™ Kit for Probes (Bio-Rad).
184 The reaction mix contained 909 nM of each primer and 227 nM of probe. The samples were placed in
185 the droplet generator using 70 µL of generator oil. The resulting picolitre droplet emulsions (40 µL)
186 were transferred to a T100 Thermal Cycler or CFX96 (Bio-Rad). The reverse transcription was
187 performed with 60 min hold at 50°C. The cDNA amplification was performed with 10 min hold at
188 95°C, 40 cycles of 95°C for 30 sec then 58°C for 60 sec with a ramp rate of 2°C per sec, followed by 10
189 min hold at 98°C and 30 min hold at 4°C, and finally the maintain of the samples at 12°C until data
190 analysis. After amplification, the plate was transferred to QX200 Droplet Reader (Bio-Rad) using QX
191 Manager Edition™ Software (Bio-Rad) to measure the number of positive and negative droplets
192 based on fluorescence amplitude. The detection limit was estimated to 2.000 copies/L.

193 Negative controls were included in each experiment to ensure no contamination and set up the
194 thresholds for considering a partition as positive. Detection specificity of variant was assessed in each
195 reaction using positive RNA controls kindly provided by Pr. Charlotte Charpentier (University Hospital
196 Center Bichat- C. Bernard, Paris, France) and Pr. Evelyne Schvoerer (CHRU Nancy, France).

197

198 **Sequencing of wastewater samples**

199 Sequencing was performed based on targeted whole genome library preparation of SARS-CoV-2
200 using the QIAseq DIRECT SARS-CoV-2 kit (QIAGEN). Five microliters of extracted RNA from each
201 sample were used to make this library. Amplicons were quantified using an ultra-sensitive
202 fluorescent nucleic acid stain for quantitating double-stranded DNA (Quant-iT™ PicoGreen® dsDNA
203 reagent, Thermo). Samples normalized at 4.0 nM were pooled into a single library and diluted to 10
204 pM concentration according to the manufacturer recommendations. Sequencing was performed with
205 the MiSeq V2 chemistry with 2 x 150 cycles according to the manufacturer's protocol. Data analysis
206 was performed using the Galaxy tools. Briefly, no quality filtering was applied, all reads were
207 considered. Reads were mapped with BWA-MEM (version 0.7.17.1) against reference genome
208 (NC_45512). Duplicate were cleaned from the BAM dataset using Mark Duplicates (version 2.18.2.2).
209 Variant calling was performed using Lofreq (version 2.1.5) and annotation of SARS-CoV-2 variants
210 using SnpEff eff version 4.5 covid19).

211

212 **Mathematical and statistical methods**

213 Dynamics of mutations (concentration or mutation frequency) were modeled based on daily average
214 concentration (when multiple locations were sampled on the same day) using a LOWESS smoothing
215 method on 10 adjacent points (GraphPad Prism v9.0), allowing to limit outlier effects. Correlations
216 between different datasets were estimated using Spearman test (GraphPad Prism v9.0). First
217 derivative of dynamics curves was calculated using dedicated function of GraphPad Prism software.
218 Normalized data were calculated by dividing raw mutation concentrations by PMMoV concentrations
219 or by daily drinking water consumption. To homogenize the scales of the graphics, the ratios were
220 multiplied by 10.000.000 or 400.000 respectively.

221

222 **Results**

223 1. *Dating of the emergence of Omicron variants in France*

224 The del 69-70 mutation of the VOC Omicron BA.1 spike protein and the L452R mutation carried by
225 the Delta VOC were quantified by digital RT-PCR on wastewater samples as early as the first week of
226 November 2021. Quantification of the D61L mutation in the ORF6, suggestive of the Omicron BA.2
227 variant, was implemented on the samples as early as mid-November 2021. The heat maps presented
228 in Figure 1 highlighted a very early detection of del69-70 mutation in samples from the Greater Paris
229 area as early as November 15, 2021 in a context of predominant Delta variant illustrated by the
230 screening of the L452R mutation. A later detection of del 69-70 was observed in the other major
231 French cities. Similarly, the D61L mutation was detected in samples from the greater Paris area as
232 early as January 3, 2022 heralding the emergence and rapid spread of the Omicron BA.2 variant. The
233 density of samples taken in the greater Paris area, both in wastewater treatment plants and sewage
234 collectors of the city of Paris, allowed to observe at first punctual detections of these mutations, then
235 the generalization of the positivity of the sampling sites was a precursor of the large diffusion of the
236 BA.1 and BA.2 lineages of the Omicron VOC in the population and to the acceleration of their
237 propagation.

238

239 2. *Dynamics of mutation in wastewater and of variant based on patient sequencing*

240 Two periods were considered and 625 samples were processed. The first period concerned the first
241 half of 2021 during which the del69-70 and L452R mutations, carried by Alpha VOC and Delta VOC
242 respectively, were quantified. The proportions of each mutation were estimated in comparison to
243 the total SARS-CoV-2 genome concentrations based on gene E quantification. This period was
244 marked by a strong predominance of del69-70 mutation suggesting Alpha VOC before decreasing
245 from April 2021. It should be noted that the L452R mutation was detected as early as January 2021
246 and could be found in nearly 15% of the circulating genomes in the wastewater. Its increasing
247 frequency from mid-April 2021 was accompanied by a decrease in the proportion of del69-70. In
248 wastewater, the L452R mutation became the majority mutation by May 27, 2021. The increase in the
249 proportion of the L452R mutation was strikingly associated with the regional dynamics of vaccination

250 (first dose) (figure 2, panel A) (Santé publique France, 2022b). Nevertheless, the concentration of
251 SARS-CoV-2 genomes in raw wastewater associated with this Delta VOC epidemic wave was greatly
252 reduced compared to the Alpha VOC wave (figure 2, panel B). These mutation dynamics were
253 compared to local open data from the national sequencing program (EMERGEN) as well (figure 2,
254 panel A) (Santé publique France, 2022b). This program was only implemented in France in mid-
255 February 2021 explaining the shape of the curve. The Delta VOC was reported for the first time
256 through sequencing from patient samples on May 10, 2021. The Delta variant became the majority of
257 clinical samples on June 21, 2021 ((Santé publique France, 2022b).

258 The second period began in November 2021, during which time Delta VOC represented 100% of
259 identified viral sequences isolated from patients sequencing (Santé publique France, 2022b) and the
260 L452R mutation was present in about 100% of circulating sequences in wastewater. The decrease of
261 the L452R mutation in wastewater, concomitant with the decrease of the Delta VOC in clinical
262 samples, started at the end of November 2021 and became a very small minority (<10% of
263 sequences) by mid-January 2022. However, this L452R mutation was still detectable in wastewater
264 by March 15, 2022 suggesting the circulation of variants carrying this mutation (Delta VOC or other
265 non-VOC variants). The del69-70 mutation was once more detected in a wastewater sample from 15
266 November 2021 in the greater Paris area. Generalization and increase of this mutation were initiated
267 at the end of November 2021 to become the majority on December 25, 2021. The growth dynamics
268 of del69-70 in wastewater were very similar to that of the Omicron VOC estimated in patient by
269 sequencing (Santé publique France, 2022b). In contrast, the del69-70 mutation began to decline by
270 mid-January 2022 in parallel with the increase of the D61L (ORF6) mutation, detected in samples as
271 early as January 3, 2022. Genomes carrying the D61L mutation became predominant by mid-
272 February 2022 to present almost all circulating genomes by March 15, 2022 in the greater Paris
273 wastewater. Sequencing results from patients did not report a distinction between Omicron BA .1
274 and BA.2 sublineages to date (Figure 2, panel C) (Santé publique France, 2022b). The association of
275 the del69-70 mutation with the Omicron BA.1 VOC was based on a polymorphism in the forward

276 primer and the absence of residual detection of this specific mutation in the summer of 2021 (data
277 not shown). During this second period, the concentration of SARS-CoV-2 genomes was also
278 compared to the regional incidence. The dynamics of the viral genome increase in wastewater that
279 preceded the dynamics of incidence was of about 13 days (Figure 2, panel D). The concentration of
280 viral genomes in wastewater resulting from the Omicron BA.1 VOC wave was much higher than those
281 related to Delta VOC. To confirm the relevance of the digital RT-PCR method, the same samples were
282 analyzed by RT-qPCR based on gene E quantification using the previously described method (Wurtzer
283 et al., 2022). Trend curves were compared and showed close relationship (supplementary data 2).

284

285 3. *Evolutionary trend: interest of raw concentration normalization*

286 Viral concentrations in wastewater can be influenced by significant population changes since raw
287 wastewater not solely comes from population (sewer cleaning, rain, water infiltration, industries...).

288 To assess the impact of human population movements on the evolutionary trends of the different
289 VOC mutations, comparison of raw mutation concentrations and normalized concentrations was
290 performed using two indicators. The first one was related to an human biomarker, the Pepper Mild
291 Mottle Virus genome (PMMoV), in wastewater. The second one was related to the consumption of
292 drinking water by the local population living in Paris, France. PMMoV genome concentration and
293 drinking water consumption were plotted in figure 3, panels A and B. Mean PMMoV genome
294 concentration ranged between 10^6 and 10^8 copies/L with a median value of about 10^7 copies/L,
295 suggesting large fluctuations. On the contrary, the volume of drinking water consumed were more
296 stable. An evolution of both parameters showed that a decrease in drinking water consumption was
297 observed during holidays (shaded period on the graph) suggesting a decrease in the population
298 connected to the watershed. Such variations were not observed with the PMMoV genome
299 concentration.

300 Both datasets underwent the same LOWESS smoothing setup over the same period. The evolutionary
301 trends of each mutation were very comparable, but some trend breaks can be observed (figure 4,

302 panel D). Since the values were relatively stable (except during holidays), normalization by drinking
303 water consumption only significantly altered the dynamics, mostly over the period of population
304 movement (figure 4, panels A and B). Normalization with PMMoV noticeably altered viral dynamics in
305 wastewater. The precocity of the viral dynamics was also reduced. This approach highlighted an
306 epidemic rebound during February 2022 before an increase in March 2022 related to Omicron BA.2
307 (figure 4, panels A and C).

308 The viral dynamics in raw wastewater having the best correlation with incidence data was
309 determined by a Spearman correlation test. Taking into account the precocity of the raw and
310 normalized curves using the drinking water consumption, these two modeling showed a very good
311 correlation with the incidence curve ($r = 0.956$; $p < 0.0001$ and $r = 0.968$; $p < 0.0001$) respectively,
312 while the correlation of the normalized curve using the PMMoV genome concentration seemed to be
313 less relevant ($r = 0.761$; $p < 0.0001$).

314 Normalization methods did not change the mutation frequencies and by the way the dynamics, but
315 slight modifications of mutation concentrations were observed (figure 4, panels A, B and C).

316

317 4. *Dynamics of variant proportions in wastewater: from Alpha to Omicron BA.2*

318 The evolutionary kinetics of each mutation suggestive of VOC were studied over the 2 time periods.
319 As PMMoV concentrations were not available for the first period and normalization by drinking water
320 consumption did not significantly modify the modeling of viral dynamics, first derivatives of the raw
321 mutation concentration trend curves were calculated to determine variant replacement rates based
322 on the mutations studied. The values are presented in Table 2. The values corresponded to maximum
323 rates of change in the proportion of mutation per day relative to the next majority population. Thus,
324 the proportion of the del69-70 mutation of Alpha VOC increased by a maximum of 2.8% per day,
325 compared with 5.2% for the L452R mutation of Delta VOC. The del69-70 mutation of Omicron BA.1
326 VOC increased by 6.0% per day in wastewater, while the D61L mutation replaced it more rapidly

327 (maximum 17.2%/day) as soon as the wave started (March 2022). The rate of decay of the del69-70
328 mutation of Omicron BA .1 VOC was similar to those of L452R mutation.

329

330 The sum of the concentrations of the mutations of interest carried by the different genomes was
331 compared with the total concentration of circulating genomes over the two periods studied. During
332 the first period, the correlation between both datasets was estimated using a Spearman test ($r =$
333 0.789 ; $p < 0.0001$) and a shift with the SARS-CoV-2 genome curve was observed suggesting the
334 circulation of other variants than Alpha and Delta circulating in the wastewater (figure 5, panel A). In
335 the second period, the sum of variants carrying the L452R, del69-70 and D61L mutations appeared to
336 be more consistent with the total concentration of circulating genomes, independently of the viral
337 concentration in wastewater ($r = 0.966$; $p < 0.0001$) suggesting less « other variants » circulating in
338 wastewater (figure 5, panel B).

339

340 5. *Comparison of mutation frequencies by digital RT-PCR and sequencing.*

341 The frequencies of del69-70, L452R, and D61L mutations were estimated by sequencing on 23
342 wastewater samples collected in the greater Paris area between December 15, 2021 and February
343 28, 2022. These mutation frequencies were compared to those estimated on the same samples by
344 digital RT-PCR (Figure 6, panel A). The SARS-CoV-2 concentrations ranged from $3.3E^{+4}$ copies/L to
345 $1.1E^{+6}$ copies/L corresponding to an input for library preparation ranging from 36 to 1,206 copies. A
346 Spearman's correlation showed a significant moderate positive correlation of mutation frequencies (r
347 $= 0.38$, $p = 0.002$). The del60-70 mutation was not found by sequencing in eight samples despite
348 including samples where Omicron BA.1 was the predominant variant and SARS-CoV-2 concentrations
349 the highest, suggesting a lower sensitivity of this sequencing-based mutation monitoring. Results also
350 showed important disparities in viral population dynamics over this period resulting from these
351 datasets (Figure 6, panels B, C and D). The fluctuations observed in the mutation frequencies by
352 sequencing have made curve smoothing difficult and the dynamics of change in majority populations

353 were not evident to discern. Mutation frequencies for each sample and sequencing depth for each
354 mutation position were available in supplementary data 3.

355

356 **Discussion**

357 Omicron VOC is at the origin of an unprecedented upsurge in cases of COVID-19 since December
358 2021 in France. In Hong Kong, where people at risk (over 80 years old) are poorly vaccinated to date,
359 a sharp increase in deaths has currently been observed (The New York Times, 2022). If Omicron VOC
360 is spreading very rapidly in the population, the vaccination coverage in France (77,8% of the
361 population with a complete vaccination schedule by March 15, 2022) may explain the lower severity
362 of this VOC and its moderate impact on the French health system, compared to previous VOC. Viral
363 spread in the general population may therefore become increasingly difficult to monitor with
364 classical epidemiological indicators. Changes in tropism relative to Omicron VOC have also been
365 reported. Nasopharyngeal swab-based screening may be less well suited to this new VOC or possible
366 future variants, potentially leading to an underestimation of real viral circulation (Gupta, 2022;
367 Marais et al., 2021).

368 Wastewater-based epidemiology allows tracking the overall dynamics of the SARS-CoV-2 epidemic
369 (Medema et al., 2020b; Randazzo et al., 2020; Wurtzer et al., 2022, 2020). Variant identification
370 results from sequencing, but such approach faces limitations for application in wastewater with
371 respect to RNA quality and quantity (Lou et al., 2022), but also mathematical tools to deconvolute
372 isolated mutations to reconstruct the original genomes in a mixture of variants (Agrawal et al.,
373 2022b; Jahn et al., 2021; Smyth et al., 2022). Different studies have shown that it is also possible to
374 monitor specific mutations suggestive of VOC to identify the emergence of VOC in a territory and to
375 explain the predominance of certain VOC in epidemic waves (Caduff et al., 2022; Carcereny et al.,
376 2022; Erster et al., 2022; Wurtzer et al., 2022). RT-qPCR approaches require calibration tools for
377 absolute quantification or allelic discrimination (wild-type vs mutated) for relative quantification.
378 Digital PCR allows more flexibility by offering a most probable number estimation (in accordance

379 with Poisson's law), by avoiding the realization of a standard curve and by allowing multiplexing of
380 reactions.

381 The del69-70 mutation was shared by Alpha and Omicron BA.1 VOCs. However, Alpha VOC has been
382 chronologically replaced by Delta VOC, to the point of disappearance as confirmed by the absence of
383 del69-70 mutation detection since summer 2021 in wastewater. In this regard, the WHO no longer
384 identifies Alpha VOC as a circulating VOC (World Health Organization, 2022). On the other hand,
385 Omicron BA.1 VOC carries the synonymous mutation C21762T, the presence of which confers a
386 better discrimination between the del69-70 mutation carried by Alpha VOC and that carried by
387 Omicron BA.1 VOC. Detection of the del69-70 mutation resulting from Alpha VOC was therefore
388 unlikely in winter 2021. To our knowledge, this study is the first to date the emergence of BA.1 and
389 BA.2 sublineages of Omicron VOC in raw wastewater in France. The Omicron BA.1 VOC was detected
390 earlier in the greater Paris area compared to other French regions. The Paris region is a transit hub
391 between the different regions and the international. This observed precocity is therefore not
392 surprising. The monitoring of specific mutations in wastewater has allowed the very early
393 identification of the Omicron BA.1 VOC (Ferré et al., 2022) as well as the BA.2 sublineage from
394 January 2022.

395 Retrospective studies have also demonstrated the presence of minor viral populations carrying the
396 L452R mutation, suggestive of Delta VOC, as early as January 2021, in parallel with the strong
397 expansion of Alpha VOC. The high transmissibility of Alpha VOC was at the origin of the third wave of
398 COVID-19 encountered in France (Wurtzer et al., 2022). The introduction of vaccination coupled with
399 acquired collective immunity to this VOC has probably allowed the expansion of an already
400 circulating and better adapted variant such as Delta VOC whose L452R mutation allows a better
401 escape to the immune response (Motozono et al., 2021). The results presented suggested that
402 vaccination (and previous infections) could have contributed to the selection of the Delta VOC but
403 also strongly reduced viral circulation with respect to the concentrations measured in the
404 wastewater when the Delta VOC was in the majority. The large increase in viral genome

405 concentration in wastewater during the Omicron BA.1 wave, compared with the Delta wave, was also
406 consistent with the reduced efficacy of the Omicron VOC vaccine response (Cele et al., 2022). These
407 results were consistent with a vaccine-induced reduction in severe forms of COVID-19 resulting from
408 Omicron VOC infection without preventing viral circulation in the populations.

409 To date, VOCs are effectively monitored by conventional epidemiological indicators and intensive
410 sequencing of strains isolated from patients. The dynamics of VOC-suggestive mutations in
411 wastewater were consistent with VOC dynamics in patients, particularly with respect to the early
412 detections, wave dynamics and changes in dominant populations. While variants may emerge
413 simultaneously (e.g. Alpha and Delta VOCs), there were no periods in which different SARS-CoV-2
414 VOCs were codominant. Over the periods studied, the co-spreading of different variants in a
415 population was finally only very transient and each variant was bound to be replaced by another one.
416 This constant variant replacement demonstrated the SARS-CoV-2 evolution spreading within a
417 population that has been largely immunized collectively either by one or more infections or by
418 vaccination. Thus, maximum VOC replacement rates were calculated for variants that have circulated
419 extensively in France since January 2021. Beta and Gamma VOCs represented at most 13.5% of the
420 sequenced strains (April 26, 2021) and their detection in wastewater was not investigated in this
421 study. The maximum VOC replacement rate for Alpha VOC (2,8%/day) was very close to the growth
422 rate (4%/day) estimated in another study (Caduff et al., 2022). It was quite remarkable that the
423 maximum replacement rate has progressively increased as new VOCs have emerged, suggesting
424 increasingly contagious variants. Furthermore, the sum of the proportions of the different targeted
425 mutations explained the majority of circulating SARS-CoV-2 genomes from November 2021 to March
426 2022. Contrary to the first studied period (from January to June 2021), the sum of the del69-70 and
427 L452R mutations only partially explained the total circulating genomes. This result was consistent
428 with the cumulative proportions of the other VOCs (e.g. Beta and Gamma VOCs) and the decreasing
429 proportion of the original strain of SARS-CoV-2, and could underline the increasing “fitness” of
430 circulating VOC.

431 In addition to the method variability (Bivins et al., 2021b, 2021a) and potentially different fecal
432 shedding depending on the variants, the SARS-CoV-2 concentrations in wastewater can be affected
433 by heavy rainfall and population movement. Mathematical algorithms have been proposed to
434 compare data sets obtained from different methods or laboratories, and to correct the raw
435 concentrations by the flow of wastewater inlet (Cluzel et al., 2022; Courbariaux et al., 2022). The
436 greater Paris area is particularly affected by the latter because it is a very touristy region, and this
437 region concentrates a very strong professional activity. This second period was strongly impacted by
438 the school vacations of Christmas (from December 20, 2021 to January 1, 2022) and winter (from
439 February 19 to March 7, 2022) during which many people leave the region. To account for these
440 population variations, PMMoV genome, a human biomarker, was also measured by digital RT-PCR as
441 well as the daily drinking water consumption in Paris. The PMMoV is a plant virus that is very
442 abundant in human stools, although the origin of this presence is not really known. Identified as
443 plant virus (pepper), food is suspected to be the main source of contamination (Colson et al., 2010).
444 Its detection has been proposed as tracer of anthropogenic activity (D'Aoust et al., 2021; Malla et al.,
445 2019). In this study, the PMMoV genome concentration in raw wastewater showed an important
446 variability that did not highlight the population movements in the studied watershed as
447 demonstrated by drinking water consumption and vacation calendar. Using population indicator such
448 as drinking water consumption or PMMoV shedding, the normalized viral dynamics in wastewater
449 were quite different. Normalization using drinking water consumption generated a curve very close
450 to the dynamics based on raw concentrations, with a more precise definition of the peak of the
451 curve. The correlation of these results with the regional incidence curve was also the best fitted. The
452 overall dynamic revealed a temporal advance in agreement with other results (Caduff et al., 2022;
453 Cluzel et al., 2022; Wurtzer et al., 2022). Nevertheless, this temporal advance on the wave related to
454 the Omicron VOC appeared to be greater than the advance reported for previous VOCs. Similar
455 advance can be observed on SARS-CoV-2 wastewater monitoring data in the U.S (Biobot.io, 2022).
456 This finding could be explained by a higher proportion of asymptomatic or paucisymptomatic

457 infections that would be detected later. Normalization based on PMMoV genome concentration
458 suggested a wave of viral genomes in wastewater synchronized with incidence. Surprisingly, this
459 approach showed a viral rebound in February 2022 that was not observed on the other modeled
460 curves, nor on the incidence curve. This observation was probably the reason for the lower
461 correlation. If other human biomarkers could be evaluated such as CrAssphages or specific F-RNA
462 phages, a previous study also concluded that normalization of SARS-CoV-2 signal by fecal indicator
463 did not improve the correlation with the incidence (Ai et al., 2021). All three approaches agreed on a
464 significant resurgence of the viral circulation observed in wastewater in early March 2022 confirmed
465 by incidence data. The circulation of variants leading to less severe infections, resulting either from
466 acquired collective immunity (vaccination and infections) or from an attenuation of the intrinsic viral
467 pathogenicity, could lead to a less good identification of the cases of infection in the populations, and
468 thus to an apparent incidence decorrelated from the real incidence. In this sense, viral monitoring in
469 wastewater will allow an unbiased approach to viral circulation.

470 This study also demonstrated the interest of monitoring specific mutations evocative of VOC because
471 of the simplicity of setting up such an measurement, its low cost and the result quickness, which are
472 indispensable for informing health authorities. This study also highlighted the limitations of
473 sequencing in wastewater with respect to analytical sensitivity that may result from the low
474 concentration of SARS-CoV-2 genomes, the very low concentration of mutations in minority variant
475 populations, insufficient sequencing depth, and non-homogeneous coverage along the entire viral
476 genome. Similar limitations have been already reported (Caduff et al., 2022). The accumulation of
477 mutations identified by sequencing is also challenged by the reconstruction of the genomes from
478 which these mutations originate. Mathematical algorithms for deconvolution of isolated mutations
479 or long fragment sequencing approaches to identify different polymorphisms in the same reads may
480 improve the predictivity of sequencing. To date, sequencing must be interpreted with caution for
481 quantitative assessments of mutation frequency in wastewater.

482

483 **Conclusion**

484 The quantification of mutations suggestive of VOCs circulating in wastewater has allowed a depiction
485 of the VOC propagation dynamics in the greater Paris area population. This approach also allowed
486 early detection of the Omicron VOC BA.1 and BA.2 lineages emergence in this area. The observed
487 dynamics confirmed that the vaccination strategy of the human population, as well as exposition of
488 previous variants, probably contributed to the selection of Delta VOC to the detriment of Alpha VOC,
489 but also to the strong decrease of the viral circulation in the human population during the same
490 period, confirming the effectiveness of the vaccine response against these VOCs. Moreover, the
491 normalization of concentrations based on the drinking water consumption in Paris seemed to be a
492 relevant method to follow the population movements in this region. This normalized approach
493 provided a viral dynamic in close relationship with the regional incidence curve. Spreading of variants
494 leading to less severe infections could also lead to a detection delay through patient-centered
495 syndromic surveillance tools. Thus, raw wastewater testing will still allow this tracking, as well as the
496 VOC dynamics monitoring during the spread of SARS-CoV-2 in populations.

497

498 **Acknowledgments**

499 We thank all the people who have made it possible to collect all these wastewater samples since the
500 beginning of the pandemic, especially the team of sewage workers of Paris, France, who set up a
501 specific monitoring. Technical teams of WWTP (SIAM, SIAAP and other utilities) should also be
502 thanked. We also thank all the people who participated in the exchange of ideas and who cannot be
503 listed as co-authors of the study.

504 * member of the scientific interest group OBEPINE : IRBA (Boni M), Eau de Paris (Wurtzer S, Moulin L),
505 Sorbonne Université (Mouchel JM, Maday Y, Marechal V), IFREMER (Le Guyader S), LCPME (Bertrand
506 I, Gantzer C).

507

508 **Funding**

509 Sample collection and nucleic acid extraction were carried on the OBEPINE Research grant (French
510 ministry of Research and French ministry of Health). Development of tools for the detection of
511 variants by digital PCR and sequencing was funded both by Eau de Paris and a grant from the
512 Emereaude project. A part of the analyses was also financially supported by the « Syndicat
513 Intercommunal du Bassin d'Arcachon ».

514

515 References

- 516 Agrawal, S., Orschler, L., Schubert, S., Zachmann, K., Heijnen, L., Tavazzi, S., Gawlik, B.M., de Graaf,
517 M., Medema, G., Lackner, S., 2022a. Prevalence and circulation patterns of SARS-CoV-2
518 variants in European sewage mirror clinical data of 54 European cities. *Water Res* 214,
519 118162. <https://doi.org/10.1016/j.watres.2022.118162>
- 520 Agrawal, S., Orschler, L., Tavazzi, S., Greither, R., Gawlik, B.M., Lackner, S., 2022b. Genome
521 Sequencing of Wastewater Confirms the Arrival of the SARS-CoV-2 Omicron Variant at
522 Frankfurt Airport but Limited Spread in the City of Frankfurt, Germany, in November 2021.
523 *Microbiol Resour Announc* 11, e0122921. <https://doi.org/10.1128/MRA.01229-21>
- 524 Ahmed, W., Bivins, A., Smith, W.J.M., Metcalfe, S., Stephens, M., Jennison, A.V., Moore, F.A.J.,
525 Bourke, J., Schlebusch, S., McMahon, J., Hewitson, G., Nguyen, S., Barcelon, J., Jackson, G.,
526 Mueller, J.F., Ehret, J., Hosegood, I., Tian, W., Wang, H., Yang, L., Bertsch, P.M., Tynan, J.,
527 Thomas, K.V., Bibby, K., Graber, T.E., Ziels, R., Simpson, S.L., 2022. Detection of the Omicron
528 (B.1.1.529) variant of SARS-CoV-2 in aircraft wastewater. *Science of The Total Environment*
529 820, 153171. <https://doi.org/10.1016/j.scitotenv.2022.153171>
- 530 Ahmed, W., Simpson, S., Bertsch, P., Bibby, K., Bivins, A., Blackall, L., Bofill-Mas, S., Bosch, A.,
531 Brandao, J., Choi, P., Ciesielski, M., Donner, E., D'Souza, N., Farnleitner, A., Gerrity, D.,
532 Gonzalez, R., Griffith, J., Gyawali, P., Haas, C., Hamilton, K., Hapuarachchi, C., Harwood, V.,
533 Haque, R., Jackson, G., Khan, S., Khan, W., Kitajima, M., Korajkic, A., Rosa, G.L., Layton, B.,
534 Lipp, E., McLellan, S., McMinn, B., Medema, G., Metcalfe, S., Meijer, W., Mueller, J., Murphy,
535 H., Naughton, C., Noble, R., Payyappat, S., Petterson, S., Pitkanen, T., Rajal, V., Reyneke, B.,
536 Roman, F., Rose, J., Rusinol, M., Sadowsky, M., Sala-Comorera, L., Setoh, Y.X., Sherchan, S.,
537 Sirikanchana, K., Smith, W., Steele, J., Sabburg, R., Symonds, E., Thai, P., Thomas, K., Tynan, J.,
538 Toze, S., Thompson, J., Whiteley, A., Wong, J., Sano, D., Wuertz, S., Xagorarakis, I., Zhang, Q.,
539 Zimmer-Faust, A., Shanks, O., 2021. Minimizing Errors in RT-PCR Detection and Quantification
540 of SARS-CoV-2 RNA for Wastewater Surveillance.
541 <https://doi.org/10.20944/preprints202104.0481.v1>
- 542 Ai, Y., Davis, A., Jones, D., Lemeshow, S., Tu, H., He, F., Ru, P., Pan, X., Bohrerova, Z., Lee, J., 2021.
543 Wastewater SARS-CoV-2 monitoring as a community-level COVID-19 trend tracker and
544 variants in Ohio, United States. *Science of The Total Environment* 801, 149757.
545 <https://doi.org/10.1016/j.scitotenv.2021.149757>
- 546 Bertrand, I., Challant, J., Jeulin, H., Hartard, C., Mathieu, L., Lopez, S., Schvoerer, E., Courtois, S.,
547 Gantzer, C., 2021. Epidemiological surveillance of SARS-CoV-2 by genome quantification in
548 wastewater applied to a city in the northeast of France: Comparison of ultrafiltration- and
549 protein precipitation-based methods. *International Journal of Hygiene and Environmental*
550 *Health* 233, 113692. <https://doi.org/10.1016/j.ijheh.2021.113692>
- 551 Biobot.io, 2022. Covid-19 Wastewater Monitoring in the U.S. [WWW Document]. URL
552 <https://biobot.io/data/>
- 553 Bivins, A., Kaya, D., Bibby, K., Simpson, S.L., Bustin, S.A., Shanks, O.C., Ahmed, W., 2021a. Variability
554 in RT-qPCR assay parameters indicates unreliable SARS-CoV-2 RNA quantification for

- 555 wastewater surveillance. *Water Res* 203, 117516.
556 <https://doi.org/10.1016/j.watres.2021.117516>
- 557 Bivins, A., North, D., Wu, Z., Shaffer, M., Ahmed, W., Bibby, K., 2021b. Within- and between-Day
558 Variability of SARS-CoV-2 RNA in Municipal Wastewater during Periods of Varying COVID-19
559 Prevalence and Positivity. *ACS EST Water* 1, 2097–2108.
560 <https://doi.org/10.1021/acsestwater.1c00178>
- 561 Boogaerts, T., Van den Bogaert, S., Van Poelvoorde, L.A.E., El Masri, D., De Roeck, N., Roosens,
562 N.H.C., Lesenfants, M., Lahousse, L., Van Hoorde, K., van Nuijs, A.L.N., Delputte, P., 2022.
563 Optimization and Application of a Multiplex Digital PCR Assay for the Detection of SARS-CoV-
564 2 Variants of Concern in Belgian Influent Wastewater. *Viruses* 14, 610.
565 <https://doi.org/10.3390/v14030610>
- 566 Caduff, L., Dreifuss, D., Schindler, T., Devaux, A.J., Ganesanandamoorthy, P., Kull, A., Stachler, E.,
567 Fernandez-Cassi, X., Beerenwinkel, N., Kohn, T., Ort, C., Julian, T.R., 2022. Inferring
568 transmission fitness advantage of SARS-CoV-2 variants of concern from wastewater samples
569 using digital PCR, Switzerland, December 2020 through March 2021. *Euro Surveill* 27.
570 <https://doi.org/10.2807/1560-7917.ES.2022.27.10.2100806>
- 571 Carcereny, A., Garcia-Pedemonte, D., Martínez-Velázquez, A., Quer, J., Garcia-Cehic, D., Gregori, J.,
572 Antón, A., Andrés, C., Pumarola, T., Chacón-Villanueva, C., Borrego, C.M., Bosch, A., Guix, S.,
573 Pintó, R.M., 2022. Dynamics of SARS-CoV-2 Alpha (B.1.1.7) variant spread: The wastewater
574 surveillance approach. *Environ Res* 208, 112720.
575 <https://doi.org/10.1016/j.envres.2022.112720>
- 576 Cele, S., Gazy, I., Jackson, L., Hwa, S.-H., Tegally, H., Lustig, G., Giandhari, J., Pillay, S., Wilkinson, E.,
577 Naidoo, Y., Karim, F., Ganga, Y., Khan, K., Bernstein, M., Balazs, A.B., Gosnell, B.I., Hanekom,
578 W., Moosa, M.-Y.S., Lessells, R.J., de Oliveira, T., Sigal, A., 2021. Escape of SARS-CoV-2
579 501Y.V2 from neutralization by convalescent plasma. *Nature* 593, 142–146.
580 <https://doi.org/10.1038/s41586-021-03471-w>
- 581 Cele, S., Jackson, L., Khoury, D.S., Khan, K., Moyo-Gwete, T., Tegally, H., San, J.E., Cromer, D.,
582 Scheepers, C., Amoako, D.G., Karim, F., Bernstein, M., Lustig, G., Archary, D., Smith, M.,
583 Ganga, Y., Jule, Z., Reedoy, K., Hwa, S.-H., Giandhari, J., Blackburn, J.M., Gosnell, B.I., Abdool
584 Karim, S.S., Hanekom, W., NGS-SA, COMMIT-KZN Team, von Gottberg, A., Bhiman, J.N.,
585 Lessells, R.J., Moosa, M.-Y.S., Davenport, M.P., de Oliveira, T., Moore, P.L., Sigal, A., 2022.
586 Omicron extensively but incompletely escapes Pfizer BNT162b2 neutralization. *Nature* 602,
587 654–656. <https://doi.org/10.1038/s41586-021-04387-1>
- 588 Chassalevris, T., Chaintoutis, S.C., Koureas, M., Petala, M., Moutou, E., Beta, C., Kyritsi, M.,
589 Hadjichristodoulou, C., Kostoglou, M., Karapantsios, T., Papadopoulos, A., Papaioannou, N.,
590 Dovas, C.I., 2022. Wastewater monitoring using a novel, cost-effective PCR-based method
591 that rapidly captures the transition patterns of SARS-CoV-2 variant prevalence (from Delta to
592 Omicron) in the absence of conventional surveillance evidence (preprint). *Epidemiology*.
593 <https://doi.org/10.1101/2022.01.28.21268186>
- 594 Cluzel, N., Courbariaux, M., Wang, S., Moulin, L., Wurtzer, S., Bertrand, I., Laurent, K., Monfort, P.,
595 Gantzer, C., Guyader, S.L., Boni, M., Mouchel, J.-M., Maréchal, V., Nuel, G., Maday, Y., 2022.
596 A nationwide indicator to smooth and normalize heterogeneous SARS-CoV-2 RNA data in
597 wastewater. *Environ Int* 158, 106998. <https://doi.org/10.1016/j.envint.2021.106998>
- 598 Colson, P., Richet, H., Desnues, C., Balique, F., Moal, V., Grob, J.-J., Berbis, P., Lecoq, H., Harlé, J.-R.,
599 Berland, Y., Raoult, D., 2010. Pepper mild mottle virus, a plant virus associated with specific
600 immune responses, Fever, abdominal pains, and pruritus in humans. *PLoS One* 5, e10041.
601 <https://doi.org/10.1371/journal.pone.0010041>
- 602 Corman, V.M., Landt, O., Kaiser, M., Molenkamp, R., Meijer, A., Chu, D.K.W., Bleicker, T., Brunink, S.,
603 Schneider, J., Schmidt, M.L., Mulders, D.G.J.C., Haagmans, B.L., van der Veer, B., van den
604 Brink, S., Wijsman, L., Goderski, G., Romette, J.-L., Ellis, J., Zambon, M., Peiris, M., Goossens,
605 H., Reusken, C., Koopmans, M.P.G., Drosten, C., 2020. Detection of 2019 novel coronavirus

606 (2019-nCoV) by real-time RT-PCR. *Euro Surveill* 25. [https://doi.org/10.2807/1560-](https://doi.org/10.2807/1560-7917.ES.2020.25.3.2000045)
607 [7917.ES.2020.25.3.2000045](https://doi.org/10.2807/1560-7917.ES.2020.25.3.2000045)

608 Courbariaux, M., Cluzel, N., Wang, S., Maréchal, V., Moulin, L., Wurtzer, S., consortium, O., Mouchel,
609 J.-M., Maday, Y., Nuel, G., 2022. A flexible smoother adapted to censored data with outliers
610 and its application to SARS-CoV-2 monitoring in wastewater. *arXiv:2108.02115* [stat].

611 Covariants.org, 2022. Overview of Variants/Mutations [WWW Document]. URL
612 <https://covariants.org/variants>

613 Crits-Christoph, A., Kantor, R.S., Olm, M.R., Whitney, O.N., Al-Shayeb, B., Lou, Y.C., Flamholz, A.,
614 Kennedy, L.C., Greenwald, H., Hinkle, A., Hetzel, J., Spitzer, S., Koble, J., Tan, A., Hyde, F.,
615 Schroth, G., Kuersten, S., Banfield, J.F., Nelson, K.L., 2021. Genome Sequencing of Sewage
616 Detects Regionally Prevalent SARS-CoV-2 Variants. *mBio* 12.
617 <https://doi.org/10.1128/mBio.02703-20>

618 D'Aoust, P.M., Mercier, E., Montpetit, D., Jia, J.-J., Alexandrov, I., Neault, N., Baig, A.T., Mayne, J.,
619 Zhang, X., Alain, T., Langlois, M.-A., Servos, M.R., MacKenzie, M., Figeys, D., MacKenzie, A.E.,
620 Graber, T.E., Delatolla, R., 2021. Quantitative analysis of SARS-CoV-2 RNA from wastewater
621 solids in communities with low COVID-19 incidence and prevalence. *Water Res* 188, 116560.
622 <https://doi.org/10.1016/j.watres.2020.116560>

623 Erster, O., Mendelson, E., Kabat, A., Levy, V., Mannasse, B., Assraf, H., Azar, R., Ali, Y., Bucris, E., Bar-
624 llan, D., Mor, O., Elul, M., Mandelboim, M., Sofer, D., Fleishon, S., Zuckerman, N.S., Bar-Or, I.,
625 2022. Specific Detection of SARS-CoV-2 Variants B.1.1.7 (Alpha) and B.1.617.2 (Delta) Using a
626 One-Step Quantitative PCR Assay. *Microbiol Spectr* e0217621.
627 <https://doi.org/10.1128/spectrum.02176-21>

628 European Centre for Disease Prevention and Control, 2022. SARS-CoV-2 variants of concern [WWW
629 Document]. URL <https://www.ecdc.europa.eu/en/covid-19/variants-concern>

630 Ferré, V.M., Peiffer-Smadja, N., Visseaux, B., Descamps, D., Ghosn, J., Charpentier, C., 2022. Omicron
631 SARS-CoV-2 variant: What we know and what we don't. *Anaesthesia Critical Care & Pain*
632 *Medicine* 41, 100998. <https://doi.org/10.1016/j.accpm.2021.100998>

633 Fontenele, R.S., Kraberger, S., Hadfield, J., Driver, E.M., Bowes, D., Holland, L.A., Faleye, T.O.C.,
634 Adhikari, S., Kumar, R., Inchausti, R., Holmes, W.K., Deitrick, S., Brown, P., Duty, D., Smith, T.,
635 Bhatnagar, A., Yeager, R.A. 2nd, Holm, R.H., von Reitzenstein, N.H., Wheeler, E., Dixon, K.,
636 Constantine, T., Wilson, M.A., Lim, E.S., Jiang, X., Halden, R.U., Scotch, M., Varsani, A., 2021.
637 High-throughput sequencing of SARS-CoV-2 in wastewater provides insights into circulating
638 variants. *Water Res* 205, 117710. <https://doi.org/10.1016/j.watres.2021.117710>

639 Graber, T.E., Mercier, É., Bhatnagar, K., Fuzzen, M., D'Aoust, P.M., Hoang, H.-D., Tian, X., Towhid, S.T.,
640 Plaza-Diaz, J., Eid, W., Alain, T., Butler, A., Goodridge, L., Servos, M., Delatolla, R., 2021. Near
641 real-time determination of B.1.1.7 in proportion to total SARS-CoV-2 viral load in wastewater
642 using an allele-specific primer extension PCR strategy. *Water Res* 205, 117681.
643 <https://doi.org/10.1016/j.watres.2021.117681>

644 Gupta, R., 2022. SARS-CoV-2 Omicron spike mediated immune escape and tropism shift. *Res Sq*
645 *rs.3.rs-1191837*. <https://doi.org/10.21203/rs.3.rs-1191837/v1>

646 Haramoto, E., Kitajima, M., Kishida, N., Konno, Y., Katayama, H., Asami, M., Akiba, M., 2013.
647 Occurrence of Pepper Mild Mottle Virus in Drinking Water Sources in Japan. *Appl. Environ.*
648 *Microbiol.* 79, 7413–7418. <https://doi.org/10.1128/AEM.02354-13>

649 Heijnen, L., Elsinga, G., de Graaf, M., Molenkamp, R., Koopmans, M.P.G., Medema, G., 2021. Droplet
650 digital RT-PCR to detect SARS-CoV-2 signature mutations of variants of concern in
651 wastewater. *Sci Total Environ* 799, 149456. <https://doi.org/10.1016/j.scitotenv.2021.149456>

652 Jahn, K., Dreifuss, D., Topolsky, I., Kull, A., Ganesanandamoorthy, P., Fernandez-Cassi, X., Bänziger, C.,
653 Stachler, E., Fuhrmann, L., Jablonski, K.P., Chen, C., Aquino, C., Stadler, T., Ort, C., Kohn, T.,
654 Julian, T.R., Beerenwinkel, N., 2021. Detection of SARS-CoV-2 variants in Switzerland by
655 genomic analysis of wastewater samples (preprint). *Infectious Diseases (except HIV/AIDS)*.
656 <https://doi.org/10.1101/2021.01.08.21249379>

- 657 Kirby, A.E., Welsh, R.M., Marsh, Z.A., Yu, A.T., Vugia, D.J., Boehm, A.B., Wolfe, M.K., White, B.J.,
658 Matzinger, S.R., Wheeler, A., Bankers, L., Andresen, K., Salatas, C., Gregory, D.A., Johnson,
659 M.C., Trujillo, M., Kannoly, S., Smyth, D.S., Dennehy, J.J., Sapoval, N., Ensor, K., Treangen, T.,
660 Stadler, L.B., Hopkins, L., 2022. Notes from the Field: Early Evidence of the SARS-CoV-2
661 B.1.1.529 (Omicron) Variant in Community Wastewater - United States, November-
662 December 2021. *MMWR Morb Mortal Wkly Rep* 71, 103–105.
663 <https://doi.org/10.15585/mmwr.mm7103a5>
- 664 Lou, E., Sapoval, N., McCall, C., Bauhs, L., Carlson-Stadler, R., Kalvapalle, P., Lai, Y., Palmer, K., Penn,
665 R., Rich, W., Wolken, M., Ensor, K.B., Hopkins, L., Treangen, T.J., Stadler, L.B., 2022. Direct
666 Comparison of RT-ddPCR and Targeted Amplicon Sequencing for SARS-CoV-2 Mutation
667 Monitoring in Wastewater (SSRN Scholarly Paper No. ID 4022373). Social Science Research
668 Network, Rochester, NY. <https://doi.org/10.2139/ssrn.4022373>
- 669 Maisa, A., Spaccaferri, G., Fournier, L., Schaeffer, J., Deniau, J., Rolland, P., Coignard, B., regional
670 COVID-19 investigation team, EMERGEN consortium, 2022. First cases of Omicron in France
671 are exhibiting mild symptoms, November 2021-January 2022. *Infect Dis Now* S2666-
672 9919(22)00036–7. <https://doi.org/10.1016/j.idnow.2022.02.003>
- 673 Malla, B., Makise, K., Nakaya, K., Mochizuki, T., Yamada, T., Haramoto, E., 2019. Evaluation of
674 Human- and Animal-Specific Viral Markers and Application of CrAssphage, Pepper Mild
675 Mottle Virus, and Tobacco Mosaic Virus as Potential Fecal Pollution Markers to River Water
676 in Japan. *Food Environ Virol* 11, 446–452. <https://doi.org/10.1007/s12560-019-09398-w>
- 677 Marais, G., Hsiao, N., Iranzadeh, A., Doolabh, D., Enoch, A., Chu, C., Williamson, C., Brink, A., Hardie,
678 D., 2021. Saliva swabs are the preferred sample for Omicron detection (preprint). *Infectious
679 Diseases (except HIV/AIDS)*. <https://doi.org/10.1101/2021.12.22.21268246>
- 680 Medema, G., Been, F., Heijnen, L., Petterson, S., 2020a. Implementation of environmental
681 surveillance for SARS-CoV-2 virus to support public health decisions: Opportunities and
682 challenges. *Current Opinion in Environmental Science & Health* 17, 49–71.
683 <https://doi.org/10.1016/j.coesh.2020.09.006>
- 684 Medema, G., Heijnen, L., Elsinga, G., Italiaander, R., Brouwer, A., 2020b. Presence of SARS-
685 Coronavirus-2 RNA in Sewage and Correlation with Reported COVID-19 Prevalence in the
686 Early Stage of the Epidemic in The Netherlands. *Environmental Science* 511–516.
- 687 Motozono, C., Toyoda, M., Zahradnik, J., Saito, A., Nasser, H., Tan, T.S., Ngare, I., Kimura, I., Uriu, K.,
688 Kosugi, Y., Yue, Y., Shimizu, R., Ito, J., Torii, S., Yonekawa, A., Shimono, N., Nagasaki, Y.,
689 Minami, R., Toya, T., Sekiya, N., Fukuhara, T., Matsuura, Y., Schreiber, G., Ikeda, T.,
690 Nakagawa, S., Ueno, T., Sato, K., 2021. SARS-CoV-2 spike L452R variant evades cellular
691 immunity and increases infectivity. *Cell Host & Microbe* 29, 1124–1136.e11.
692 <https://doi.org/10.1016/j.chom.2021.06.006>
- 693 Official Journal of the European Union, 2021. Commission Recommendation (EU) 2021/472 of 17
694 March 2021 on a common approach to establish a systematic surveillance of SARS-CoV-2 and
695 its variants in wastewaters in the EU [WWW Document]. URL
696 <http://data.europa.eu/eli/reco/2021/472/oj>
- 697 Pérez-Cataluña, A., Cuevas-Ferrando, E., Randazzo, W., Falcó, I., Allende, A., Sánchez, G., 2021.
698 Comparing analytical methods to detect SARS-CoV-2 in wastewater. *Science of The Total
699 Environment* 758, 143870. <https://doi.org/10.1016/j.scitotenv.2020.143870>
- 700 Planas, D., Veyer, D., Baidaliuk, A., Staropoli, I., Guivel-Benhassine, F., Rajah, M.M., Planchais, C.,
701 Porrot, F., Robillard, N., Puech, J., Prot, M., Gallais, F., Gantner, P., Velay, A., Le Guen, J.,
702 Kassis-Chikhani, N., Edriss, D., Belec, L., Seve, A., Courtellemont, L., Péré, H., Hocqueloux, L.,
703 Fafi-Kremer, S., Prazuck, T., Mouquet, H., Bruel, T., Simon-Lorière, E., Rey, F.A., Schwartz, O.,
704 2021. Reduced sensitivity of SARS-CoV-2 variant Delta to antibody neutralization. *Nature*
705 596, 276–280. <https://doi.org/10.1038/s41586-021-03777-9>
- 706 Randazzo, W., Cuevas-Ferrando, E., Sanjuan, R., Domingo-Calap, P., Sanchez, G., 2020. Metropolitan
707 wastewater analysis for COVID-19 epidemiological surveillance. *International Journal of
708 Hygiene and Environmental Health* 230. <https://doi.org/10.1016/j.ijheh.2020.113621>

- 709 Rios, G., Lacoux, C., Leclercq, V., Diamant, A., Lebrigand, K., Lazuka, A., Soyeux, E., Lacroix, S., Fassy,
710 J., Couesnon, A., Thiery, R., Mari, B., Pradier, C., Waldmann, R., Barbry, P., 2021. Monitoring
711 SARS-CoV-2 variants alterations in Nice neighborhoods by wastewater nanopore sequencing.
712 *Lancet Reg Health Eur* 10, 100202. <https://doi.org/10.1016/j.lanepe.2021.100202>
- 713 Santé publique France, 2022a. Surveillance nationale des cas de syndrome inflammatoire multi-
714 systémique pédiatrique (PIMS) [WWW Document]. URL
715 [https://www.santepubliquefrance.fr/etudes-et-enquetes/surveillance-nationale-des-cas-de-](https://www.santepubliquefrance.fr/etudes-et-enquetes/surveillance-nationale-des-cas-de-syndrome-inflammatoire-multi-systemique-pediatrique-pims)
716 [syndrome-inflammatoire-multi-systemique-pediatrique-pims](https://www.santepubliquefrance.fr/etudes-et-enquetes/surveillance-nationale-des-cas-de-syndrome-inflammatoire-multi-systemique-pediatrique-pims)
- 717 Santé publique France, 2022b. Geo données en Santé publique [WWW Document]. URL
718 <https://geodes.santepubliquefrance.fr/>
- 719 Smyth, D.S., Trujillo, M., Gregory, D.A., Cheung, K., Gao, A., Graham, M., Guan, Y., Guldenpfennig, C.,
720 Hoxie, I., Kannoly, S., Kubota, N., Lyddon, T.D., Markman, M., Rushford, C., San, K.M.,
721 Sompanya, G., Spagnolo, F., Suarez, R., Teixeira, E., Daniels, M., Johnson, M.C., Dennehy, J.J.,
722 2022. Tracking cryptic SARS-CoV-2 lineages detected in NYC wastewater. *Nat Commun* 13,
723 635. <https://doi.org/10.1038/s41467-022-28246-3>
- 724 The New York Times, 2022. Why Omicron is so deadly in Hong Kong [WWW Document]. URL
725 [https://www.nytimes.com/2022/03/18/opinion/omicron-created-a-perfect-storm-in-hong-](https://www.nytimes.com/2022/03/18/opinion/omicron-created-a-perfect-storm-in-hong-kong.html)
726 [kong.html](https://www.nytimes.com/2022/03/18/opinion/omicron-created-a-perfect-storm-in-hong-kong.html)
- 727 Wibmer, C.K., Ayres, F., Hermanus, T., Madzivhandila, M., Kgagudi, P., Lambson, B.E., Vermeulen, M.,
728 van den Berg, K., Rossouw, T., Boswell, M., Ueckermann, V., Meiring, S., von Gottberg, A.,
729 Cohen, C., Morris, L., Bhiman, J.N., Moore, P.L., 2021. SARS-CoV-2 501Y.V2 escapes
730 neutralization by South African COVID-19 donor plasma (preprint). *Immunology*.
731 <https://doi.org/10.1101/2021.01.18.427166>
- 732 World Health Organization, 2022. Tracking SARS-CoV-2 variants [WWW Document]. URL
733 <https://www.who.int/activities/tracking-SARS-CoV-2-variants/tracking-SARS-CoV-2-variants>
- 734 Wurtzer, S., Marechal, V., Mouchel, J., Maday, Y., Teyssou, R., Richard, E., Almayrac, J., Moulin, L.,
735 2020. Evaluation of lockdown effect on SARS-CoV-2 dynamics through viral genome
736 quantification in waste water, Greater Paris, France, 5 March to 23 April 2020.
737 *Eurosurveillance* 25. <https://doi.org/10.2807/1560-7917.ES.2020.25.50.2000776>
- 738 Wurtzer, S., Waldman, P., Levert, M., Cluzel, N., Almayrac, J.L., Charpentier, C., Masnada, S., Gillon-
739 Ritz, M., Mouchel, J.M., Maday, Y., Boni, M., Marechal, V., Moulin, L., 2022. SARS-CoV-2
740 genome quantification in wastewaters at regional and city scale allows precise monitoring of
741 the whole outbreaks dynamics and variants spreading in the population. *Science of The Total*
742 *Environment* 810, 152213. <https://doi.org/10.1016/j.scitotenv.2021.152213>
- 743 Yaniv, K., Ozer, E., Lewis, Y., Kushmaro, A., 2021. RT-qPCR assays for SARS-CoV-2 variants of concern
744 in wastewater reveals compromised vaccination-induced immunity. *Water Res* 207, 117808.
745 <https://doi.org/10.1016/j.watres.2021.117808>
- 746

747

748

749 Table 1. Oligonucleotides used for detecting SARS-CoV-2 and VOCs

Oligonucleotides	Sequence	gene	VOC	reference
E_Sarbeco_F1	ACAGGTACGTTAATAGTTAATAGCGT	<i>E</i>	SARS-CoV-2	(Corman et al., 2020)
E_Sarbeco_R2	ATATTGCAGCAGTACGCACACA			
E_Sarbeco_P1	FAM-ACACTAGCCATCCTTACTGCGCTTCG-BHQ 1			
Alpha_del69-70_F186	TACTTGGTTCATGCTATCT	<i>Spike</i>	Alpha	(Wurtzer et al., 2022)
del69-70_R340	ACTGGGTCTTCGAATCTAA			
del69-70_Ps307	HEX-AGAAGTCTAACATAATAAGAGGCTGGA-BHQ 1			
BA.1_del69-70_F186_omicron	TACTTGGTTCATGTTATCT	<i>Spike</i>	Omicron BA.1	this study
del69-70_R340	ACTGGGTCTTCGAATCTAA			
del69-70_Ps307	HEX-AGAAGTCTAACATAATAAGAGGCTGGA-BHQ 1			
Delta_L452R_F22894_MAMA	GGTTGGTGGTAATTATAATTAtCG	<i>Spike</i>	Delta	this study
Delta_L452R_R22979	GTGCTACCGCCTGATA			
Delta_L452R_P22930	Cy5-TAGGAAGTCTAATCTCA-NFQ-MGB			
BA.2_F27367	GAGCAACCAATGGAGATTCTCT	ORF 6	Omicron BA.2	this study
BA.2_R27473	CCTCTAACACACTCTTGGTAGTG			
BA.2_P27416	TAMRA-TGGCACTGATAACACTCGCTACTTGTG-BHQ2			
PMMV-FP1	GAGTGGTTTGACCTTAACGTTTGA	<i>Replicase</i>	PMMoV	(Haramoto et al., 2013)
PMMV-RP1	TTGTGCGTTGCAATGCAAGT			
PMMV-Probe	ROX-CCTACCGAAGCAAATG-NFQ-MGB			

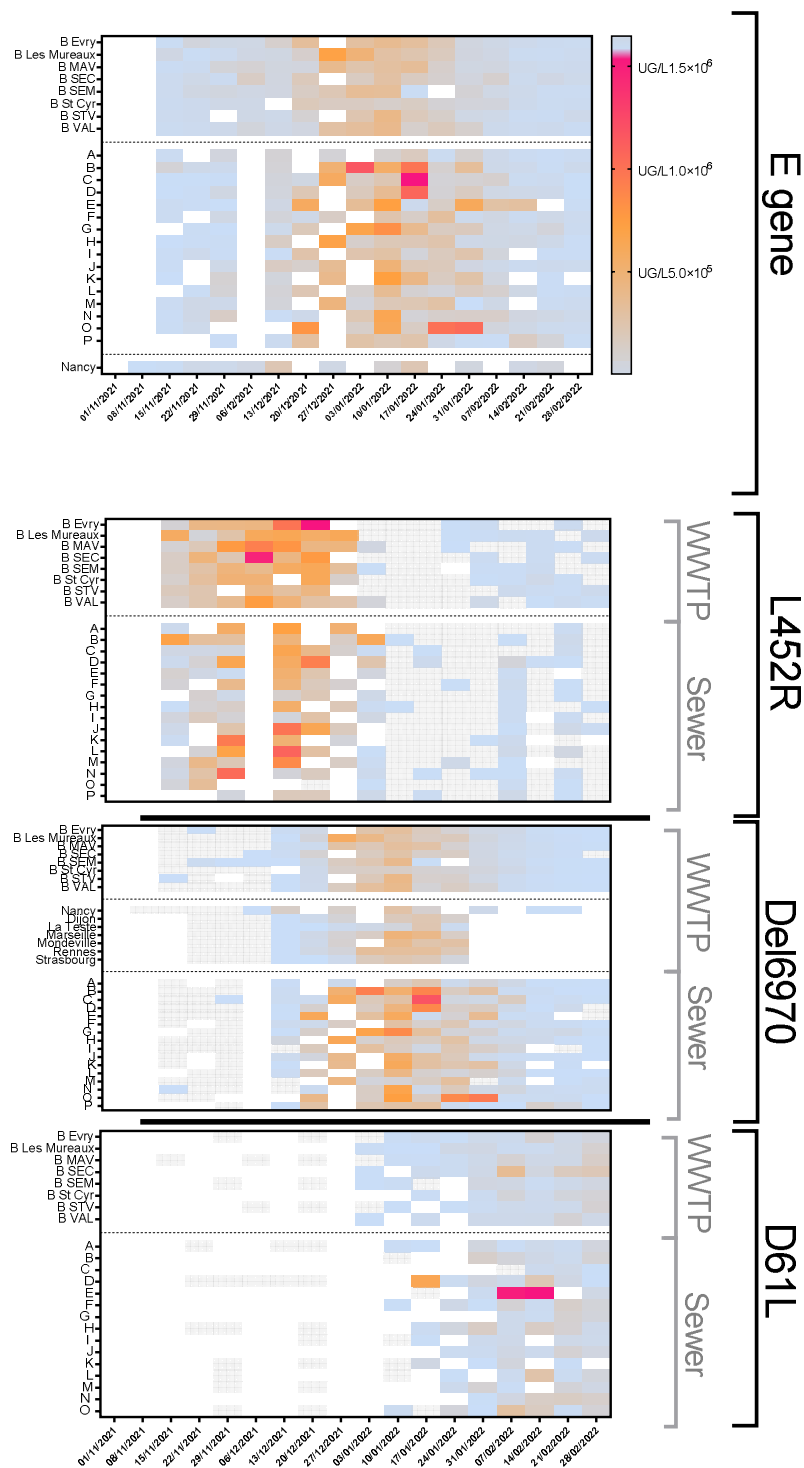
750

751 Table 2. Maximal replacement rate (RR) of variant in wastewater. RR+ indicated the replacement rate
 752 during the increase of mutation frequency, whereas RR- provided information on the decay rate of
 753 the frequency. Values were indicated in increase or decrease of frequencies per day.

VOC	Alpha	Delta	Omicron BA.1	Omicron BA.2
Mutation	del 69-70	L452R	del 69-70	D61L
RR ⁺	0.028	0.052	0.060	0.172
RR ⁻	-0.036	-0.076	-0.072	NA

754

755



756

757 Figure 1. Early detection of VOC-evocative mutation in the greater Paris area and other French
 758 regions from mid-November, 2021 to mid-March, 2022. Wastewater treatment plants (WWTP) and
 759 sewers in Paris, France were sampled twice a week. Heat-maps showed the concentration of total
 760 SARS-CoV-2 genomes and those carrying specific mutations (L452R mutation for Delta VOC, del69-70
 761 for Omicron BA.1 VOC, and D61L for Omicron BA.2 VOC). White box meant not analyzed, gray box
 762 meant not detected.

763 Figure 2. Dynamics of specific mutations in wastewater in greater Paris area from January 2021 to
764 March 2022.

765 Panel A: Frequency evolution of the del69-70 (red curve) and L452R (blue curve) mutations in
766 wastewater from January 2021 to July 2021. The red area indicated the evolution of Alpha VOC by
767 sequencing in clinical samples, the blue area for the evolution of Delta VOC. The dotted curve
768 indicated the evolution of vaccination (percentage of people receiving the first dose).

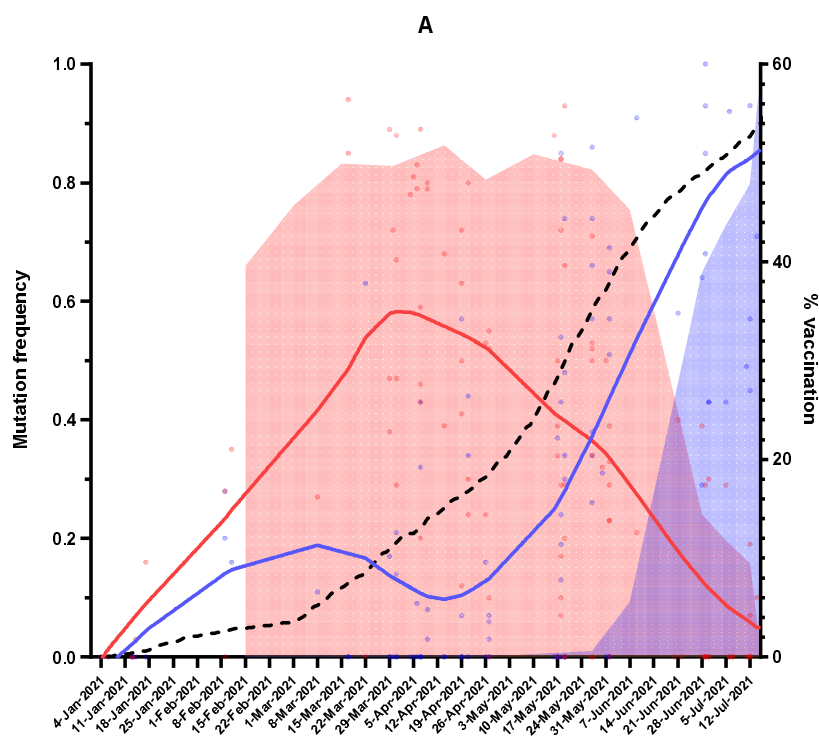
769 Panel B: Concentration evolution of the del69-70 (red curve) and L452R (blue curve) mutations, and
770 of the total SARS-CoV-2 genomes (grey curve) in wastewater from January 2021 to July 2021. The
771 dotted curve indicated the evolution of vaccination (percentage of people receiving the first dose).

772 Panel C: Frequency evolution of the L452R (blue curve), del69-70 (orange curve) and D61L (green
773 curve) mutations in wastewater from November 2021 to March 2022. The blue area indicated the
774 evolution of Delta VOC by sequencing in clinical samples, the orange area for the evolution of
775 Omicron VOC (distinction of BA.1 and BA.2 lineages was not available). The dotted curve indicated
776 the evolution of the vaccination (percentage of people receiving the first dose).

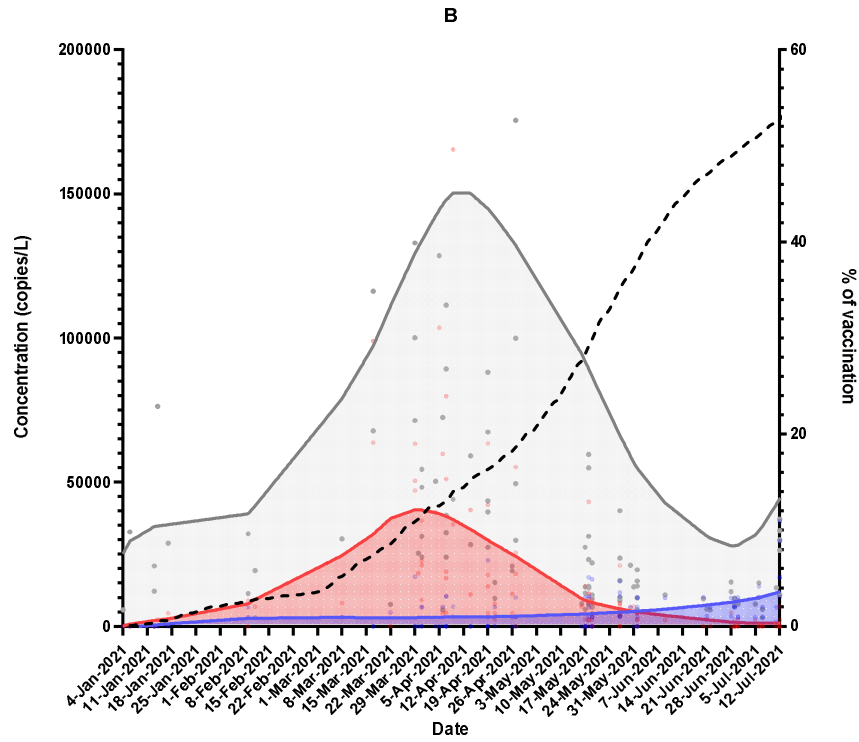
777 Panel D: Concentration evolution of the L452R (blue curve), del69-70 (orange curve) and D61L (green
778 curve) mutations, and of the total SARS-CoV-2 genomes (grey curve) in wastewater from November
779 2021 to March 2022. The dotted curve indicated the evolution of the regional incidence.

780

781



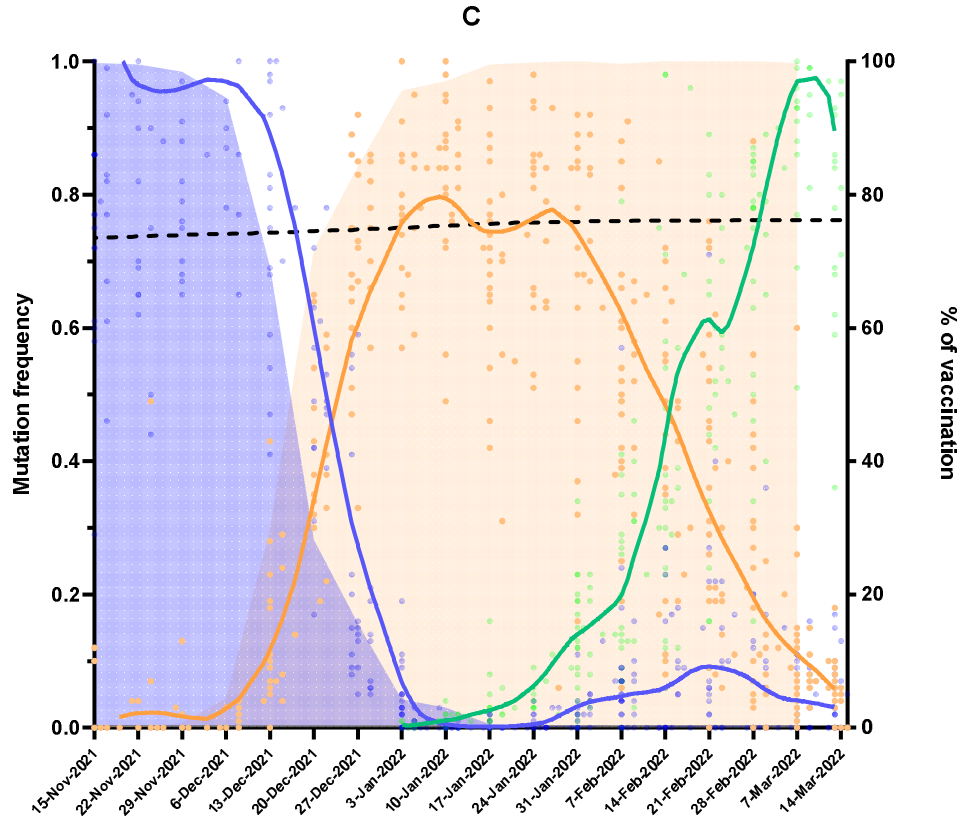
782



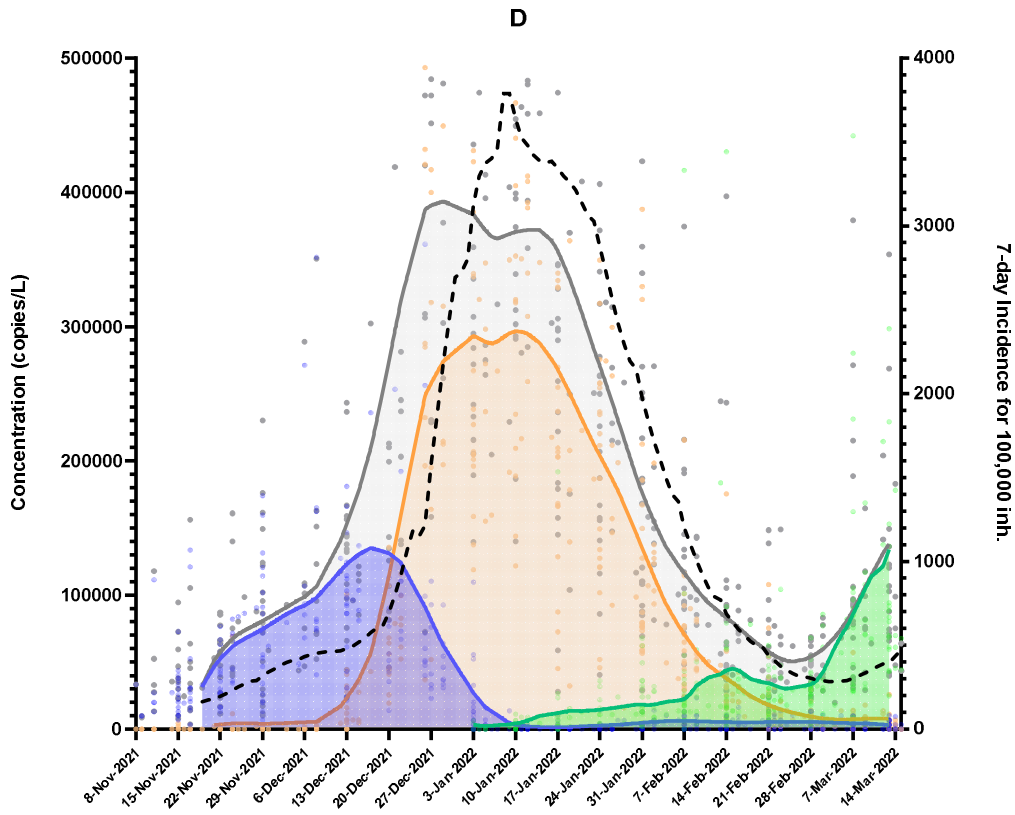
783

784

785



786



787

788

789

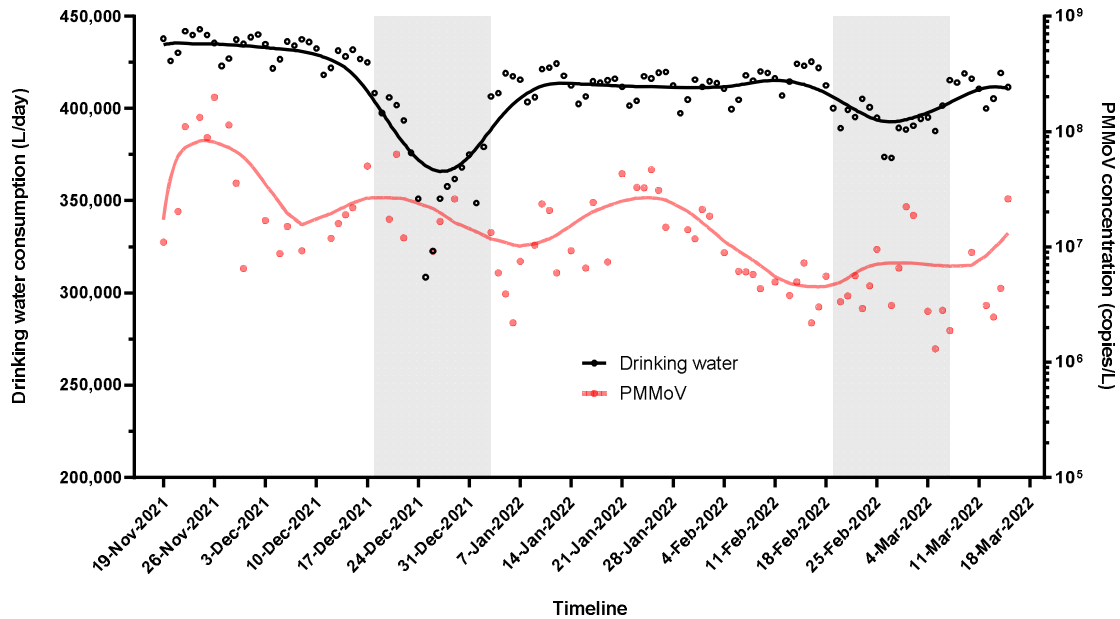
790 Figure 3. Evolution of human population indicators from November 2021 to March 2022.

791 Panel A: Drinking water consumption in Paris, France (black curve) and PMMoV concentration in
792 wastewater (red curve) were plotted, the grey areas indicated the vacation calendar.

793 Panel B: Dispersion of drinking water consumption in Paris, France and PMMoV concentration in
794 wastewater. Box and whiskers (minimum and maximum) were plotted.

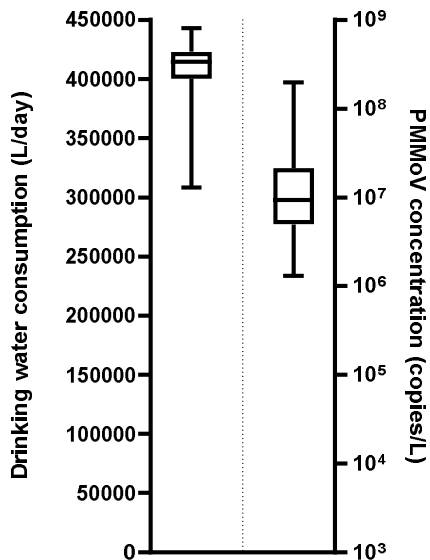
795

796 A



797

798 B



799

800 Figure 4. Evolutionary trends of the L452R (blue curve), del69-70 (orange curve) and D61L (green curve) mutation concentrations, and the total SARS-CoV-2 genome concentration (grey curve) in
801 wastewater in greater Paris area from November 2021 to March 2022. The dotted curve indicated
802 the evolution of the regional incidence.
803

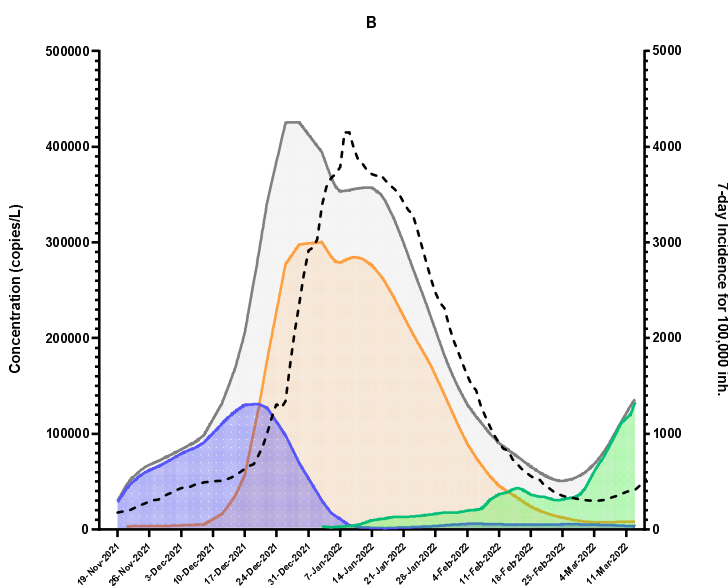
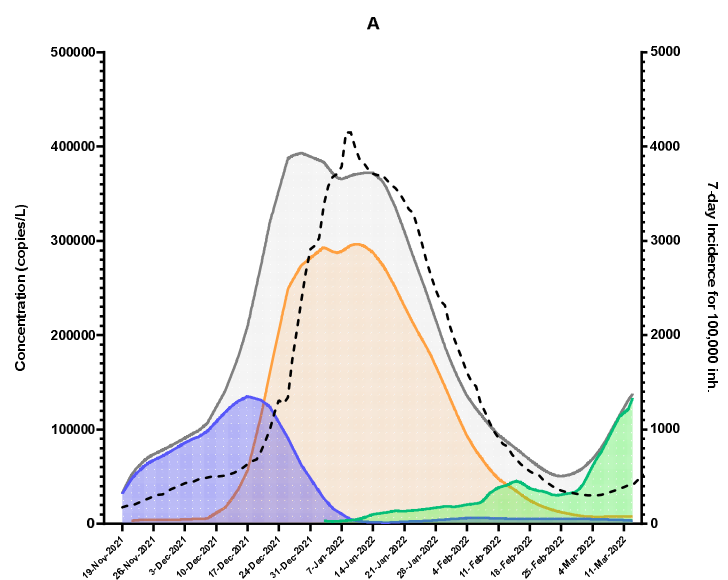
804 Panel A: trends based on raw concentrations.

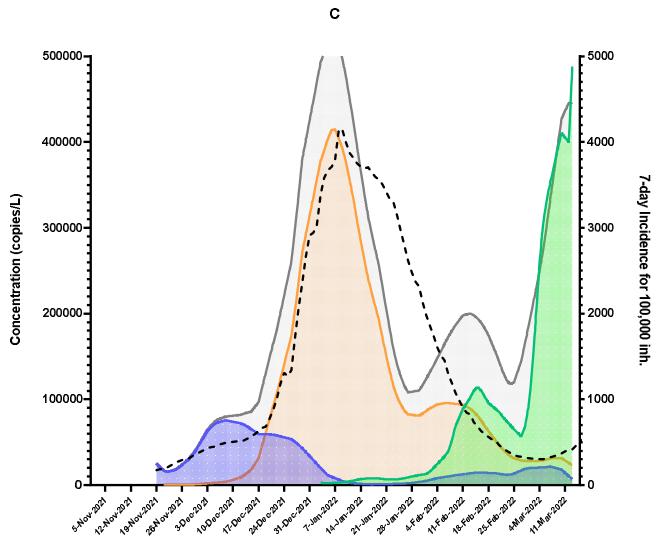
805 Panel B: trends based on concentrations normalized using drinking water consumption.

806 Panel C: trends based on concentrations normalized using PMMoV concentrations measured in
807 wastewater.

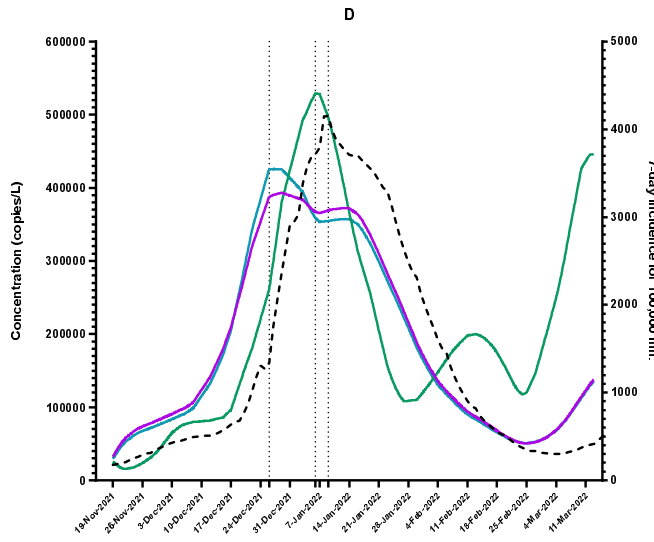
808 Panel D: Comparison of these 3 models and the incidence curve

809





812



813

814

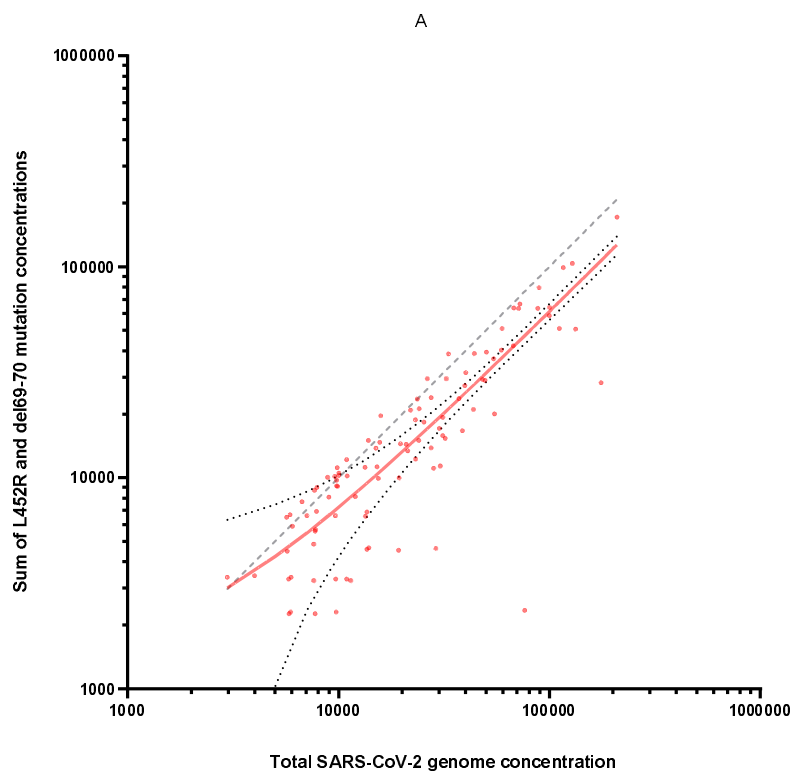
815 Figure 5. Correlation between the total SARS-CoV-2 genome concentration and the sum of VOC-
816 suggestive mutations in wastewater in the greater Paris area.

817 Panel A: Total SARS-CoV-2 genome concentrations were compared to the concentration sum of
818 del69-70 and L452R mutations measured from January 2021 to July 2021. Grey dotted line indicated
819 the theoretical correlation whereas the red line was the linear regression and the 95% confidence
820 bands of the best-fit line.

821 Panel B: Total SARS-CoV-2 genome concentrations were compared to the concentration sum of
822 del69-70, L452R and D61L mutations measured from November 2021 to March 2022. Grey dotted
823 line indicated the theoretical correlation whereas the red line was the linear regression and the 95%
824 confidence bands of the best-fit line.

825

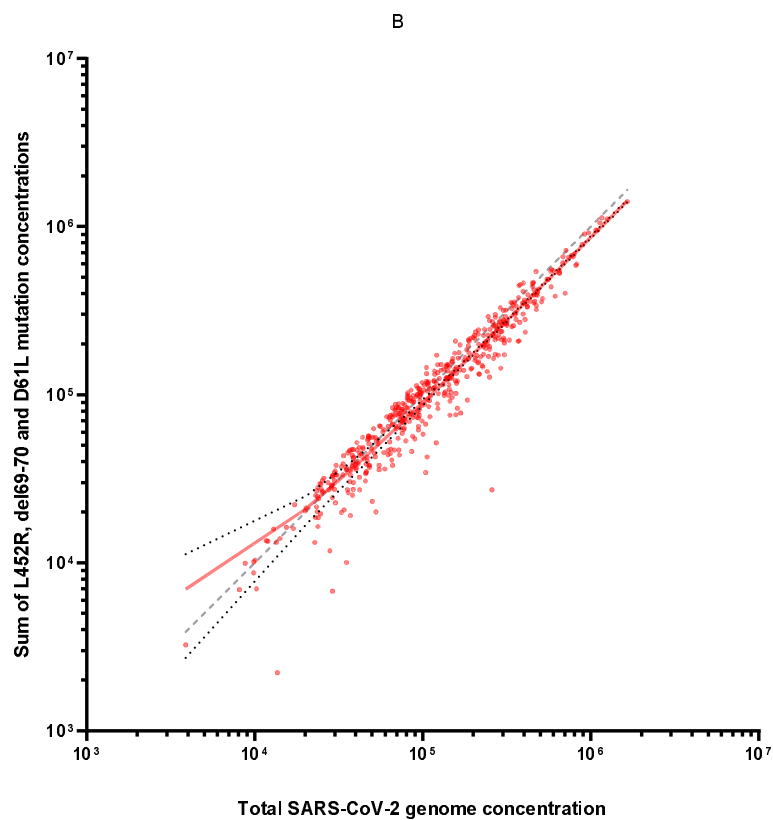
826



827

828

829



830

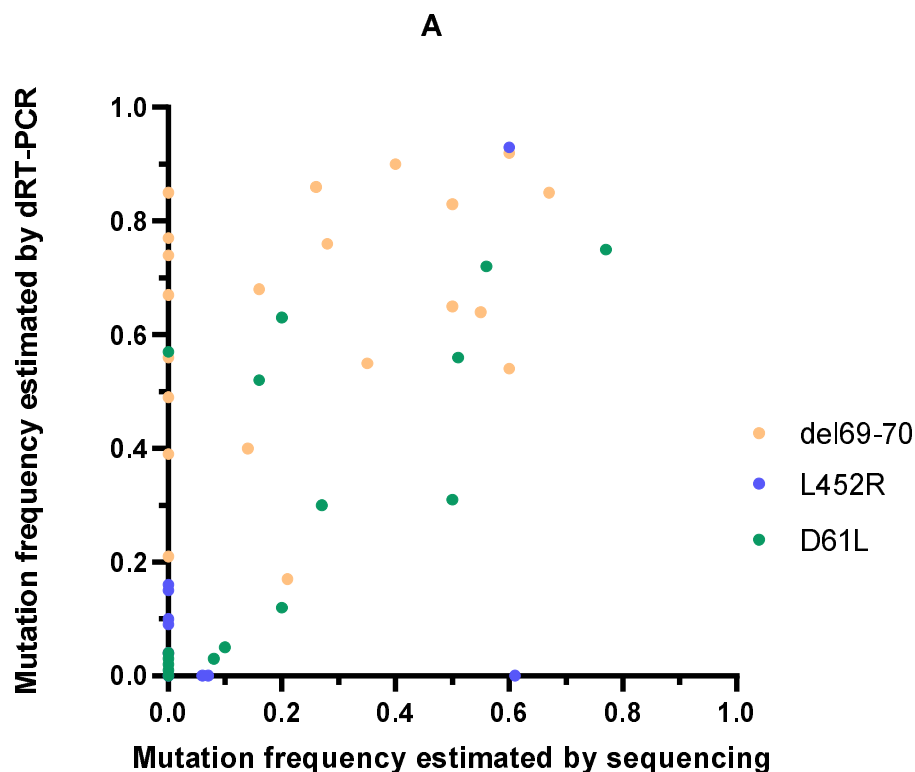
831 Figure 6. Comparison between mutation frequencies estimated by digital PCR and by sequencing in
832 wastewater samples from december 15, 2021 to February 28, 2022.

833 Panel A: Correlations estimated for the del69-70 (orange), L452R (blue) and D61L (green)

834 Panel B: Evolutionary dynamics based on the del69-70 (orange) mutation frequency determined by
835 digital PCR (solid line) or sequencing (dotted line) in wastewater.

836 Panel C: Evolutionary dynamics based on the L452R (blue) mutation frequency determined by digital
837 PCR (solid line) or sequencing (dotted line) in wastewater.

838 Panel D: Evolutionary dynamics based on the D61L (green) mutation frequency determined by digital
839 PCR (solid line) or sequencing (dotted line) in wastewater.

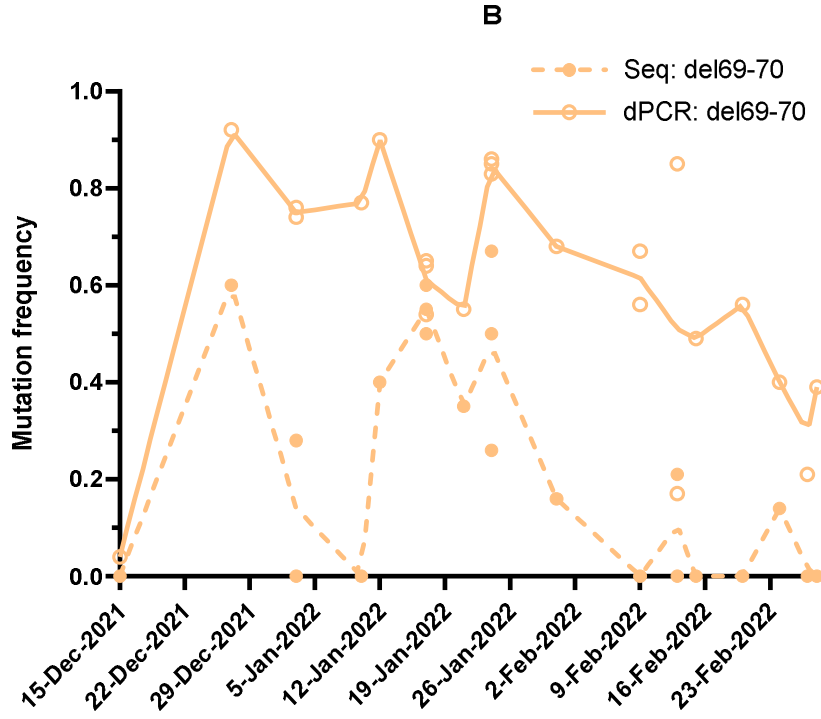


840

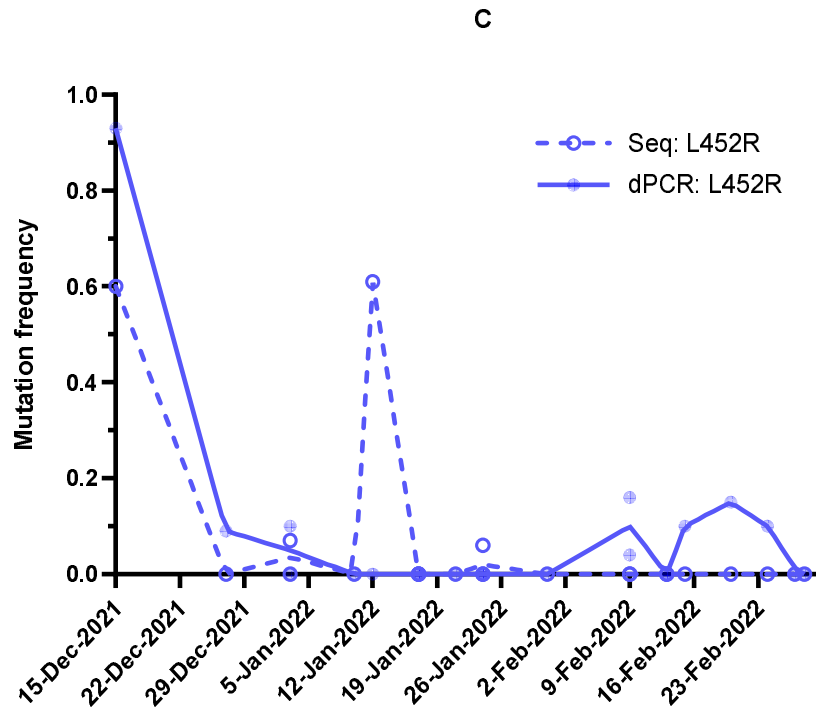
841

842

843

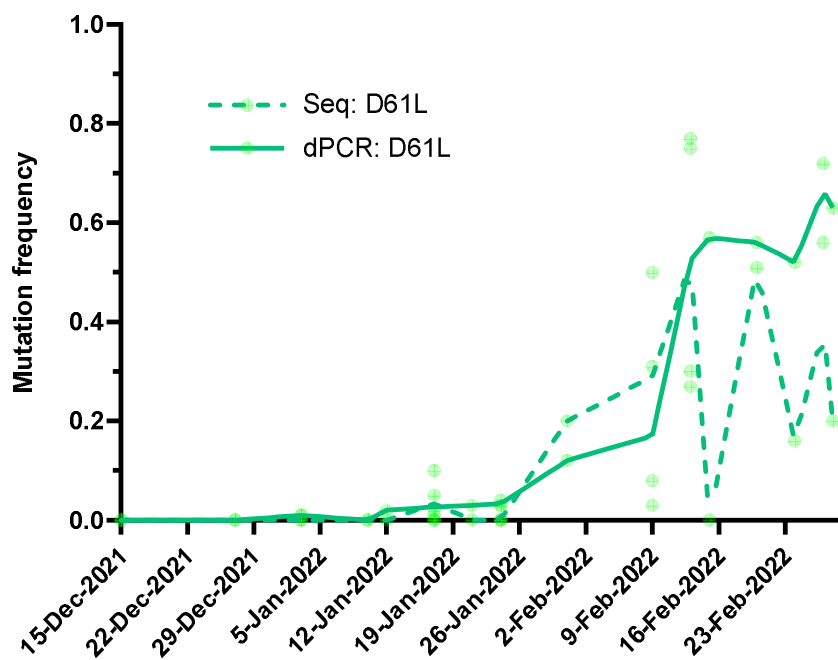


844



845

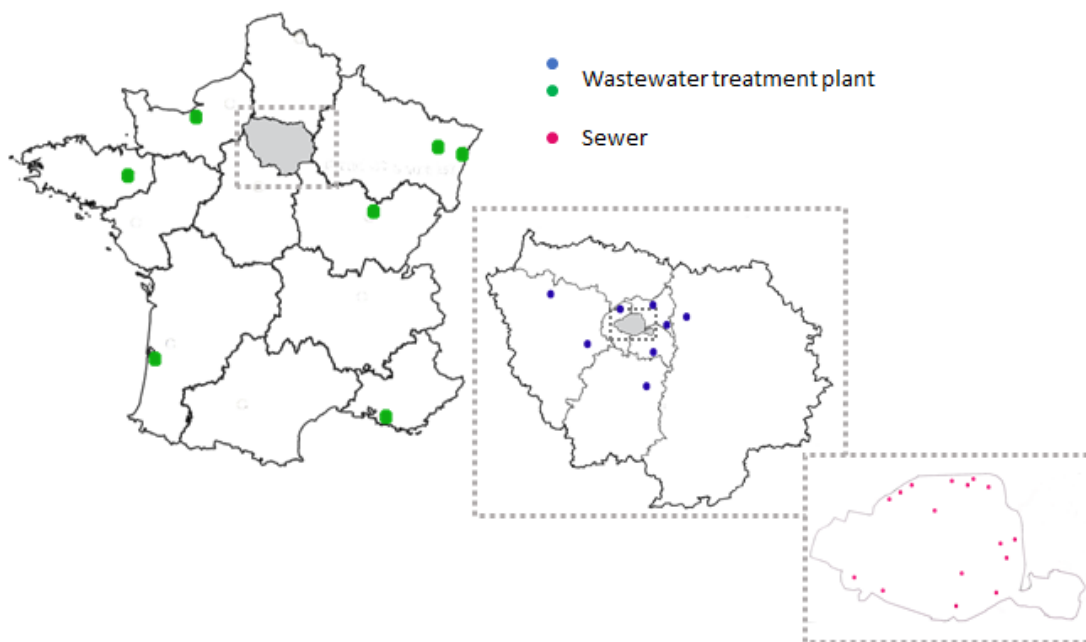
D



846

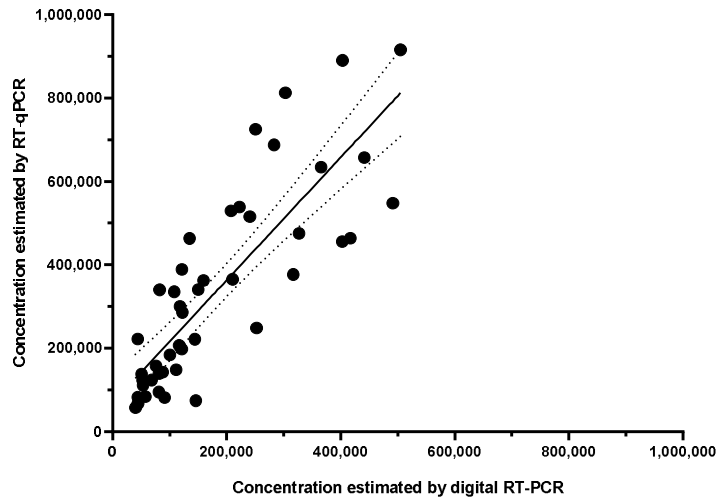
847

848 Supplementary data 1. Location of wastewater treatment plants or sewer sampled.



849

850 Supplementary data 2. Comparison between quantification by digital RT-PCR and RT-qPCR



851

852 Supplementary data 3. Mutation frequencies estimated by sequencing or digital RT-PCR (per sample)

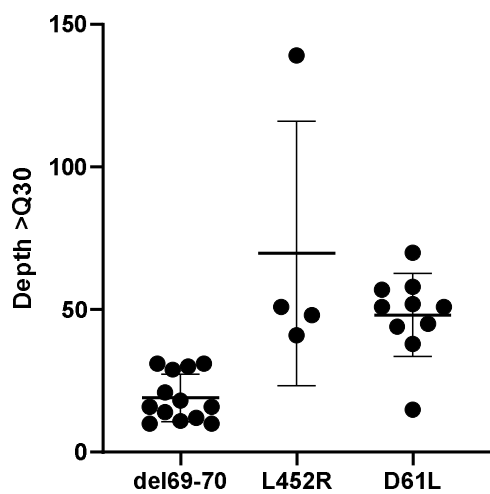
853

date	Seq: del69-70	Seq: L452R	Seq: D61L	dPCR: del69-70	dPCR: L452R	dPCR: D61L
15/12/2021	0,00	0,60	0,00	0,04	0,93	0,00
27/12/2021	0,60	0,00	0,00	0,92	0,09	0,00
03/01/2022	0,28	0,00	0,00	0,76	0,10	0,01
03/01/2022	0,00	0,07	0,00	0,74	0,00	0,01
10/01/2022	0,00	0,00	0,00	0,77	0,00	0,00
12/01/2022	0,40	0,61	0,00	0,90	0,00	0,02
17/01/2022	0,60	0,00	0,00	0,54	0,00	0,02
17/01/2022	0,55	0,00	0,00	0,64	0,00	0,01
17/01/2022	0,50	0,00	0,10	0,65	0,00	0,05
21/01/2022	0,35	0,00	0,00	0,55	0,00	0,03
24/01/2022	0,26	0,06	0,00	0,86	0,00	0,03
24/01/2022	0,67	0,00	0,00	0,85	0,00	0,04
24/01/2022	0,50	0,00	0,00	0,83	0,00	0,03
31/01/2022	0,16	0,00	0,20	0,68	0,00	0,12
09/02/2022	0,00	0,00	0,08	0,56	0,16	0,03
09/02/2022	0,00	0,00	0,50	0,67	0,04	0,31
13/02/2022	0,00	0,00	0,27	0,85	0,00	0,30
13/02/2022	0,21	0,00	0,77	0,17	0,00	0,75
15/02/2022	0,00	0,00	0,00	0,49	0,10	0,57
20/02/2022	0,00	0,00	0,51	0,56	0,15	0,56
24/02/2022	0,14	0,00	0,16	0,40	0,10	0,52
27/02/2022	0,00	0,00	0,56	0,21	0,00	0,72
28/02/2022	0,00	0,00	0,20	0,39	0,00	0,63

854

855

856 Depth sequencing for specific mutation locations.



857

858